Severed Links: Infrastructure Rigidity and the Trade Consequences of Climate Shocks

Minhao Chen* Lin William Cong†

Haoyu Gao‡ Jiaren Lu‡

First draft: Oct 2025; this draft: Jan 2026.

Abstract

Modern production networks rely on specific transport infrastructure, rendering global value chains susceptible to climate-induced capacity constraints. We isolate the trade consequences of these bottlenecks in the Yangtze River Basin, where inland exports play a crucial role in connecting inland regions to global markets, yet they are increasingly vulnerable to climate-induced disruptions. This study investigates the impact of drought on inland exports, focusing on the Yangtze River Basin's waterway transport system. Using granular data on firm-factory-port level exports and climate conditions, we find that route-specific drought exposure imposes binding constraints that significantly reduce export volumes. This effect operates by increasing logistical frictions, such as longer port stays, slower sailing speeds, and compressed loading capacities. These frictions raise shadow costs and financial constraints. Constrained by infrastructure rigidity, firms adapt through second-best reallocations—adjusting inventories, rerouting shipments, and reallocating sales to domestic markets—with minimal changes to production processes.

Keywords: Climate Change, Exports, Inland Waterway Transport, Drought
JEL Classification: F14, F18, Q54, R40

*Shenzhen Audencia Financial Technology Institute, Shenzhen University. Email: chenmh@szu.edu.cn.

†Nanyang Technological University NBS & CCDS, ABFER, CEPR, and NBER. Email: will.cong@ntu.edu.sg.

‡School of Finance, Renmin University of China. Emails: gaohaoyu@ruc.edu.cn and lujiaren03@ruc.edu.cn, respectively.

1 Introduction

Modern production networks are characterized by deep interconnectivity, where local idiosyncratic shocks can propagate rapidly across global supply chains (Acemoglu *et al.*, 2015; Barrot & Sauvagnat, 2016). While a growing literature documents how these shocks transmit through input-output linkages, the physical transport infrastructure that mediates these flows is often treated merely as a marginal cost parameter or a frictionless endowment. This abstraction overlooks a critical vulnerability: transport modes are often specific factors with limited short-run substitutability. When a climate shock disrupts a critical transport artery, it does not simply raise trade costs; it imposes a binding capacity constraint on the network. In the presence of infrastructure rigidity—where firms cannot cost-effectively switch between transport modes—such disruptions can sever market access, forcing firms into second-best resource allocations that generate significant efficiency losses.

Climate change is increasingly acting as a systemic disruptor of this physical connectivity. Unlike heatwaves or floods that primarily degrade local factor productivity or destroy physical assets, hydrological droughts operate as distinct connectivity shocks. By reducing water levels in inland waterways, droughts compress the effective capacity of shipping networks without necessarily damaging production facilities (or port infrastructure?). For industries reliant on low-cost waterborne transport—typically those trading heavy, low-value-to-weight commodities—the waterway is not just one of many options but a non-substitutable input. Consequently, a drought shock transforms into a quantity rationing mechanism: as navigable depth decreases, the infrastructure' s capacity to clear markets collapses, creating a logistical squeeze that cannot be resolved through price adjustments alone.

We examine the economic consequences of this infrastructure rigidity in the context of the Yangtze River Basin, the world's busiest inland waterway system and a central artery of China' s export machine. This setting provides an ideal natural laboratory to isolate the transport channel of climate shocks from production effects. The Yangtze serves as a logistical backbone connecting a vast inland hinterland to global markets, yet it exhibits high modal lock-in: for many upstream manufacturers, railway and road alternatives are either capacity-constrained or prohibitively expensive. Leveraging a unique dataset that merges high-frequency hydrological and vessel-movement data (AIS) with granular firm-level export records, we exploit route-specific variations in drought exposure to identify how infrastructure bottlenecks propagate to trade outcomes. This allows us to test whether firms adapt to severed links through efficient intermodal substitution or, conversely, are forced into suboptimal adjustments due to infrastructure rigidity.

To guide our empirical strategy, we develop a stylized framework that characterizes inland waterway transport not merely as a marginal cost parameter, but as a specific

factor subject to capacity rationing. We posit a complementarity between export production and logistics services, where drought imposes a binding upper limit on the aggregate capacity of the waterway network. Crucially, we introduce the assumption of infrastructure rigidity: due to prohibitive fixed costs of intermodal substitution in the short run, firms are effectively locked into the waterway network . Consequently, a drought shock manifests as a rising shadow cost of congestion (λ) rather than a simple price adjustment. Since firms are price-takers in global markets, this shadow wedge forces a quantity adjustment—reducing exports to satisfy the tightened capacity constraint—and compels a second-best reallocation of output toward domestic sales or inventory accumulation .

To precisely identify the impact of severed links, we construct a multi-dimensional database linking climate, geography, and firm behavior. First, we adopt the grid-level monthly Standardized Precipitation Evapotranspiration Index ($SPEI$) which captures the balance between precipitation and potential evapotranspiration, allowing for precise characterization of the spatiotemporal evolution of drought at the grid scale. Second, we merge the Chinese Industrial Enterprise Database with the Chinese Customs Import and Export Database to construct a unique multi-dimensional panel dataset structured as "firm-production factory–export customs port-year." For each "factory-port" pair, we calculate the shortest navigable waterway route, which defines the relevant inland waterway path connecting these two nodes. Our core measure, route-based drought exposure ($DroughtExp$), is defined by the most drought-exposed grid cell along a route composed of multiple grid cells, capturing the idea that a disruption at a single point can reduce the effective capacity of the entire route. This approach leverages the geography of the transport network to create a plausibly exogenous source of variation in firms' access to low-cost shipping. We interpret $DroughtExp$ not merely as a weather variable, but as a proxy for the effective capacity of the specific factor—the inland waterway—upon which these firms rely.

Furthermore, to identify the core transmission channel through which route-based drought affects trade, we integrate three types of high-frequency data: first, hydrological monitoring data at river cross-sections, used to directly reflect river depth and its variation over time; second, throughput data for ports along the Yangtze River, used to measure port operational intensity under varying drought exposure conditions; and third, Automatic Identification System (AIS) trajectory data, which we analyze to capture drought-induced impacts on waterway efficiency by examining vessel dwell times and sailing speeds at specific ports and river segments.

Our baseline analysis quantifies the trade destruction caused by these infrastructure bottlenecks. Estimates from our granular "firm–factory–port–year" panel reveal a substantial sensitivity to climatic constraints: a one-standard-deviation increase in route-specific drought exposure precipitates a 22% contraction in export volumes.This result holds across multiple robustness checks, including using alternative drought measures,

adjusting sample selection criteria, and controlling for potential confounders such as upstream river discharge and local drought conditions at factory locations. A placebo test in the Yellow River basin—where waterway navigability is negligible and firms rely on road/rail—shows no effect, confirming that our results are driven by the specific channel of inland shipping rather than general macro-climatic trends.

Crucially, decomposing the margins of adjustment validates the theoretical mechanism of quantity rationing. Consistent with a small open economy model featuring binding capacity constraints, we detect no significant pass-through of the shock to export unit prices. Since firms are price-takers in global markets, they cannot transfer the rising shadow cost of congestion to buyers. Instead, the adjustment is borne entirely by physical quantities: drought exposure significantly compresses the average cargo load per shipment. This dichotomy—price rigidity coupled with collapsing shipment sizes—provides direct evidence that the market clears through a "logistical squeeze" rather than price signals, forcing firms to ration their access to global markets.

We trace how hydrological anomalies propagate through the logistics network to alter firm-level fundamentals. Our analysis focuses on three distinct layers of propagation. First, we provide micro-evidence on the physical transmission channel. Utilizing high-frequency AIS vessel-tracking data, we establish that droughts act as a negative productivity shock to the shipping sector. We document that reduced river depth creates severe efficiency wedges: it forces vessels to reduce sailing speeds and extends port stay durations. Consistent with our specific-factor framework, these frictions are non-linear and most acute for deep-draft vessels, which face binding navigability constraints earlier than smaller craft .

Second, we demonstrate how these physical frictions materialize into firm-level accounting costs. We find that exposure to bottleneck-induced congestion translates into a significant spike in sales and administrative expenses. This result confirms that the theoretical shadow cost of congestion is not merely an implicit constraint but manifests explicitly as elevated operational expenditures and risk premiums required to manage logistical uncertainty .

Finally, we identify financial constraints as a critical amplifier of these real shocks. We show that the export contraction is disproportionately concentrated among firms with limited access to external finance. For these constrained agents, the drought imposes a "double bind": it simultaneously inflates operational costs (liquidity demand) while disrupting the revenue stream needed to service them. Lacking the liquidity buffers to smooth this supply chain rupture, credit-constrained firms are forced to retrench their export activities more aggressively, highlighting the destabilizing interaction between environmental volatility and financial frictions .

We examine how firms optimize under these severed links. Consistent with our theoretical premise of modal lock-in, we find virtually zero intermodal substitution: firms do

not switch to rail or road transport even under severe drought conditions . This failure of arbitrage confirms that inland waterway transport functions as a non-substitutable specific factor for these exporters. Using a sector-level waterway dependency index constructed from China's input-output tables, we find that firms in highly shipping-dependent industries (such as bulk commodities) suffer more pronounced negative effects during drought periods. Meanwhile, by employing a large language model (LLM) to classify products based on their time sensitivity, we further show that firms producing time-sensitive goods—such as products with short shelf lives or a high degree of customization—experience larger declines in exports during droughts. Consequently, the trade destruction is structurally determined by firm characteristics: the shock transmission is amplified for firms with high logistics intensity (waterway dependence) and those producing time-sensitive goods , for whom the "shadow cost of delay" is prohibitive.

Constrained by this infrastructure rigidity, firms are forced into second-best resource reallocations. We document a dichotomy in adjustment margins: while production plans remain rigid in the short run , firms substitute intertemporally by accumulating inventories and spatially by diverting output to domestic markets . Crucially, the efficacy of these buffers is limited by product attributes: inventory accumulation acts as a hedge for non-time-sensitive goods, but fails for time-sensitive products where shelf-life constraints bind immediately .

Lastly, we identify a specific margin of spatial optimization within the logistics network. While firms exhibit spatial rigidity in production—they rarely shift output across factories—they actively engage in "route arbitrage" by rerouting export flows to alternative customs ports with lower drought exposure . This route substitution effect serves as the primary logistical buffer, allowing firms to bypass localized bottlenecks even as aggregate network capacity shrinks.

Our contributions are in three aspects. First, we contribute to the literature on shock propagation by characterizing transportation networks as a specific factor subject to capacity rationing, distinct from standard production linkages. While existing studies extensively document shock transmission through input-output matrices (Acemoglu *et al.*, 2015; Barrot & Sauvagnat, 2016; Carvalho *et al.*, 2021; Acemoglu & Tahbaz-Salehi, 2024), we establish that drought shocks create infrastructure bottlenecks that impose binding capacity constraints on the network. This finding complements Chiovelli *et al.* (2025), who link physical barriers to market access; however, we differentiate by demonstrating that climate-induced barriers function as dynamic quantity rationing shocks that sever critical nodes. Consistent with Brancaccio *et al.* (2025), who emphasize transportation supply rigidities, we provide micro-level evidence that inland waterway droughts create severe capacity constraints. These constraints trigger a "logistical squeeze" that effectively crowds out trade opportunities as firms compete for diminished capacity. By framing climate risk as a disruptor of spatial connectivity, we extend the insights of Känzig &

Raghavan (2025) on global shipping choke points to domestic networks, highlighting infrastructure reliability as a critical determinant of trade resilience.

Second, we advance the literature on climate change and international trade by isolating connectivity shocks from productivity shocks. Existing studies have predominantly examined the effects of climate change on trade through the production side, documenting how climate shocks reshape trade patterns by altering agricultural productivity, comparative advantage, and related economic fundamentals (Costinot *et al.*, 2016; Nath, 2025; Waldinger, 2025). We deviate from this focus by identifying infrastructure connectivity —specifically inland waterway shipping—as a distinct transmission channel. Our analysis provides causal evidence that climate-induced disruptions to transport arteries can independently impose shadow costs of congestion that severe market access. In doing so, we highlight transportation infrastructure not merely as a passive trade cost parameter, but as a source of systemic vulnerability.

Third, we contribute to the literature on climate change adaptation. A central theme in this literature is how economic agents adjust to realized or anticipated climate impacts, with existing studies documenting adaptation at the levels of governments, households, and firms (Balboni, 2025; Hong *et al.*, 2023; Chaijaroen, 2019; Bernstein *et al.*, 2022). More recently, a growing firm-level literature shows that firms adapt to climate risks along multiple dimensions. For example, firms adjust long-term investment and production processes following extreme weather losses (Benincasa *et al.*, 2024), alter capital structure in response to climate uncertainty (Al-Ayyoub & Phan, 2026), and modify output and technology choices to mitigate productivity losses from environmental stress (Hansen-Lewis, 2026). These studies suggest that firm adaptation extends beyond damage mitigation to encompass financing, production, and technological decisions. We complement this literature by examining firm responses to climate shocks occurring along transportation routes rather than at production sites. Using micro-level data, we document how firms adjust across multiple margins, including production and operations, transportation and supply chain organization, and market participation, thereby providing new evidence on firm adaptation to climate-induced disruptions in logistics networks.

The remainder of the paper is organized as follows. Section 2 details the institutional background of the Yangtze River Basin and the nature of hydrological shocks. Section 3 outlines a conceptual framework characterizing inland transport as a specific factor subject to capacity rationing. Section 4 describes the construction of our granular firm-route-climate dataset. Section 5 presents the baseline estimates of the drought-induced export contraction and validates the mechanism of quantity rationing through price-quantity decomposition. Section 6 dissects the transmission channels, tracing the shock from physical vessel impediments to firm-level cost and financial constraints. Section 7 investigates firm adaptation strategies, highlighting the limits of intermodal substitution and the prevalence of second-best resource reallocations. Section 8 concludes.

2 Institutional Background

2.1 The Transport Network and Customs Administration

China has an extensive coastline and a world-class system of ports, and has long ranked among the world's largest trading nations. According to statistics from the General Administration of Customs and the Ministry of Transport, China's merchandise exports reached RMB 25.45 trillion in 2024, with approximately 95 percent of cargo volume transported by sea. Against this backdrop, inland waterway transport serves as a critical inland extension of the maritime supply chain, playing a central role in connecting inland regions with coastal areas and linking domestic markets to the global economy.

The Yangtze River basin spans China's western hinterland and its eastern coastal region and constitutes the world's busiest inland waterway system. According to data from the Yangtze River Navigation Administration, cargo throughput at mainline Yangtze ports reached 4.02 billion tons in 2024, ranking first globally among inland waterways for twenty consecutive years. As shown in Figure 1, by 2017 the Yangtze River's freight volume already exceeded the combined throughput of the world's five other largest inland waterways. As the principal logistics artery connecting inland China to coastal regions, the Yangtze River transport system plays an indispensable role in supporting export trade. Within this system, the Port of Shanghai serves as the primary maritime gateway, occupying a pivotal position in the transshipment of foreign trade goods. As illustrated in Figure 2, exports through the Shanghai customs district accounted for 85.1 percent, 78.2 percent, and 97.4 percent of total exports from the Yangtze River basin in 2000, 2006, and 2013, respectively, underscoring its dominant role in the basin's export activity.

Exports from the Yangtze River basin rely heavily on a "water-to-water transshipment" model. Under this arrangement, exporting firms, after completing customs clearance procedures, use feeder vessels to transfer cargo seamlessly from inland river ports to coastal ports. Relative to transport modes that depend exclusively on land-based logistics, water-to-water transshipment substantially reduces both transportation and time costs, while strengthening the functional integration between inland and coastal ports within the basin. At present, the share of water-to-water transshipment at the Port of Shanghai has consistently exceeded 50 percent and continues to rise, indicating that the majority of exports routed through coastal ports rely on inland waterway transport as a critical upstream segment of the logistics chain. By directly linking inland and coastal ports via waterways, this arrangement creates an integrated river-sea transport system that connects inland production to international shipping networks.

2.2 Climate Shocks

As climate change intensifies, extreme weather events—including heavy precipitation, prolonged heatwaves, and severe droughts—have become increasingly frequent, posing significant challenges to the stability of trade and the operating environment of the Yangtze River basin. Disruptions to the Yangtze shipping system caused by climatic anomalies have been documented historically. In January 1959, for instance, the Taixing section of the Yangtze experienced an episode of "river drying" which interrupted the main navigation channel.[1] More recently, the extreme drought of 2006 brought persistent high temperatures and unusually low rainfall to Chongqing and Sichuan. Summer precipitation in both regions fell to its lowest level since 1951, while average temperatures reached historical highs. Water levels at the Chongqing hydrological station dropped below the lowest level recorded in over a century, severely disrupting inland waterway transport.[2] The 2022 drought—the most severe in nearly half a century—further underscored the vulnerability of the system. As the Yangtze connects inland manufacturing hubs like Chongqing and Wuhan with major coastal ports like Shanghai, its disruption had substantial economic repercussions. Following the August drought, container export volumes along the river declined by 8 percent, and the transit time from Chongqing to Shanghai tripled.[3] Physically, inflows to the Xinglong hydropower hub on the Han River declined by nearly half, rendering sections of the river non-navigable. Water levels across both the main stem of the Yangtze and its tributaries fell markedly below normal, causing widespread vessel congestion in areas such as Xinglong on the Han River and Yinpan on the Wu River.[4] These disruptions led to shipment delays and interruptions in input supplies for firms along the river, highlighting the susceptibility of inland waterway transport to extreme climatic shocks.

To study these phenomena and their implications for trade, we construct a multidimensional micro-level dataset. For climate conditions, we draw on the CRU TS dataset provided by Harris *et al.* (2020), which contains gridded monthly measures of precipitation and potential evapotranspiration covering the period from 1971 to 2024. These data are used to characterize climate changes in the Yangtze River basin. As shown in Figure 3, annual precipitation exhibits pronounced fluctuations around its mean and substantial interannual variation throughout the sample period, indicating persistent precipitation instability. In contrast, both annual temperature and potential evapotranspiration display a sustained upward trend, consistent with significant warming over time.

[1] https://sk.taizhou.gov.cn/skpj/kpzs/art/2024/art_8fb8e921adc74e65933f9dea6fac6c38.html

[2] https://www.chinanews.com.cn/kong/news/2010/03-26/2192105.shtml

[3] https://www.atlanticcouncil.org/blogs/econographics/climate-drought-and-the-disrupted-future-of-global-trade/

[4] https://swj.wuhan.gov.cn/tzdt/jcss/202211/t20221125_2102612.html

Building on these data, we construct the Standardized Precipitation-Evapotranspiration Index ($SPEI$) to quantify drought exposure and climatic water balance, based on the dynamic relationship between precipitation and potential evapotranspiration. The index is computed using the Geographic and Meteorological Analysis (GMA) Python package. Focusing on our sample period (2000-2013), Figure 4 demonstrates a statistically significant downward trend in SPEI across all timescales (1, 3, 6, and 12 months), with slopes ranging from -0.024/yr to -0.052/yr, indicating a progressive intensification of drought severity. Our baseline measure of drought exposure is the one-month SPEI, as this horizon is better suited to capturing the immediate effects of short-term climatic anomalies on navigability, and thus aligns more closely with the high-frequency dynamics of firms' export decisions.

3 Conceptual Framework

To guide our empirical analysis, we develop a stylized model of firm decision-making under infrastructure constraints. Unlike standard trade models that treat transport frictions merely as iceberg costs, we characterize inland waterway transport as a specific factor subject to capacity rationing. This distinction is crucial: while cost shocks typically induce price adjustments, capacity shocks under infrastructure rigidity lead to quantity rationing and forced reallocations.

3.1 Model Setup

Consider a representative firm i that produces a final good Q using labor and capital. The firm faces a resource constraint where total output is allocated across three channels: exports (q_x), domestic sales (q_d), and inventory accumulation (q_h):

$$Q = q_x + q_d + q_h \tag{1}$$

Accessing the international market requires specific logistics services, denoted by T. We assume a complementarity between export goods and logistics services:

$$T = \alpha \cdot q_x \tag{2}$$

where $\alpha > 0$ represents the "logistics intensity" of the product. Heavier or bulkier goods (e.g., commodities) are characterized by a higher α, implying a greater reliance on physical transport capacity.

We model drought not as a marginal cost shock, but as a hard constraint on the aggregate capacity of the waterway network. The maximum transport service available

to the firm, $\bar{K}(S)$, is a decreasing function of drought severity S:

$$T \leq \bar{K}(S), \quad \text{with } \bar{K}'(S) < 0 \tag{3}$$

When drought intensifies, the navigable depth decreases, imposing a binding upper limit on the volume of goods that can be shipped.

Firms have the option to switch to an alternative transport mode, denoted by T_{alt} (e.g., rail). However, this substitution entails a substantial fixed switching cost, F, arising from contract renegotiation and logistical adjustments. We assume that for the typical firm in our sample—particularly those trading low-value-to-weight bulk commodities—this fixed cost is prohibitively high in the short run ($F \to \infty$). Consequently, firms are effectively locked in to the waterway network.[5]

The assumption of prohibitive switching costs is grounded in two stylized facts of the Yangtze River Economic Belt. First, the cost differential is structural. Industry data indicate that waterway freight rates in the region are approximately one-fifth of railway rates and one-fourteenth of road transport rates.[6] For low-margin sectors such as coal and ore, switching modes would render trade unprofitable. Second, "last-mile" connectivity remains a bottleneck. Many industrial parks along the river lack direct railway access, necessitating costly intermediate handling and trucking.[7]

3.2 The Optimization Problem

Taking the international price P^* as exogenous (small open economy assumption) and domestic revenue $R(q_d)$ as strictly concave, the firm maximizes current profits subject to the production and logistics constraints. We introduce $V(q_h)$ to denote the intertemporal value of inventory (e.g., expected future sales), assuming $V' > 0$ and $V'' < 0$. Formally, the firm's optimization problem is:

$$\max_{q_x, q_d, q_h} \Pi = P^* q_x + R(q_d) + [V(q_h) - \Phi(q_h)] - C(Q) \tag{4}$$

subject to the resource constraint (1) and the capacity constraint $\alpha q_x \leq \bar{K}(S)$.

The Lagrangian for this problem is:

$$\mathcal{L} = P^* q_x + R(q_d) + [V(q_h) - \Phi(q_h)] - C(q_x + q_d + q_h) + \lambda \left[\bar{K}(S) - \alpha q_x\right] \tag{5}$$

Where $C(\cdot)$ is the production cost, $\Phi(q_h)$ represents inventory holding costs, and λ is the

[5] We provide empirical evidence supporting the prohibitively high switching costs in the subsequent analysis.

[6] See Tianfeng Securities Research Report (2022), available at https://pdf.dfcfw.com/pdf/H3_AP202206171572699411_1.pdf.

[7] Official documents from the local government highlight the lack of rail-water intermodal connectivity as a critical issue (Jingchu Network, 2016; see news.cnhubei.com/xw/zw/201606/t3650091.shtml).

Lagrange multiplier associated with the waterway capacity constraint. The multiplier λ represents the shadow cost of congestion. It measures the marginal profit the firm effectively forfeits due to its inability to ship one additional unit of export goods.

3.3 Equilibrium and Shadow Costs

The first-order conditions with respect to q_x, q_d, and q_h yield the following equilibrium relationships:

$$\frac{\partial \mathcal{L}}{\partial q_x} = P^* - C'(Q) - \alpha\lambda = 0 \tag{6}$$

$$\frac{\partial \mathcal{L}}{\partial q_d} = R'(q_d) - C'(Q) = 0 \tag{7}$$

$$\frac{\partial \mathcal{L}}{\partial q_h} = V'(q_h) - \Phi'(q_h) - C'(Q) = 0 \tag{8}$$

Combining these conditions allows us to characterize the market clearing mechanism through a unified arbitrage condition:

$$\underbrace{P^* - \alpha\lambda(S)}_{\text{Effective Export Rev.}} = \underbrace{R'(q_d)}_{\text{Domestic MR}} = \underbrace{V'(q_h) - \Phi'(q_h)}_{\text{Net Inventory Value}} = C'(Q) \tag{9}$$

Equation (9) illuminates the central mechanism of our paper. In normal times, the capacity constraint is slack ($\lambda = 0$), and marginal revenues are equalized across markets. However, under severe drought ($S \uparrow$), the constraint becomes binding ($\bar{K}(S) < \alpha q_x^*$), causing the shadow cost $\lambda(S)$ to rise strictly above zero.

Since the firm is a price taker (P^* is fixed), it cannot pass this shadow wedge to global buyers. Instead, the rise in λ reduces the effective marginal revenue of exports. To restore equilibrium, the firm must lower the marginal revenues in the domestic and inventory channels, which implies an increase in quantities q_d and q_h.

3.4 Theoretical Predictions

This simple framework yields four testable predictions that map directly to our empirical findings.

Prediction 1: Quantity Rationing (The Extensive Margin). When the drought shock hits, the binding capacity constraint forces a reduction in export volumes. Crucially, because the adjustment is driven by the shadow cost wedge ($\alpha\lambda$) rather than a shift in global demand or explicit freight rates, we expect to see a sharp decline in quantities but no significant change in export unit prices.

Prediction 2: Propagation of Shadow Costs. Although λ is implicit, it manifests as a "friction cost" in the firm's operations. We expect drought exposure to correlate with higher operational expenses, reflecting extended dwell times and coordination efforts.

Prediction 3: Infrastructure Lock-in. Despite the rising shadow cost λ, firms will not switch to alternative transport modes (rail/road) as long as the efficiency loss ($\alpha\lambda q_x$) remains smaller than the fixed switching cost F. Given the specificity of inland water transport for bulk goods, we predict a failure of intermodal substitution.

Prediction 4: Second-Best Reallocation. Equation (9) proves that as the export channel is blocked ($q_x \downarrow$), the firm reallocates resources to substitute markets. Specifically, to equate marginal returns, the firm will divert output to domestic markets ($q_d \uparrow$) and accumulate inventory ($q_h \uparrow$).

4 Data

4.1 Variable Descriptions

4.1.1 Firm Trade Indicators

Firm-level data in this study are constructed by matching two authoritative administrative datasets: the China Industrial Enterprises Database (CIED) and the China Customs Database (CCD), covering the period from 2000 to 2013. The CIED, maintained by the National Bureau of Statistics, provides detailed information on firms' financial conditions and production activities. It includes all industrial firms whose annual main business revenue exceeds the official reporting threshold (RMB 5 million prior to 2011 and RMB 20 million thereafter). The dataset covers approximately two million firms, accounting for about 90 percent of total industrial sales during the sample period. The CCD records all export transactions conducted by Chinese firms. In addition to core transaction information, such as trade value, quantity, and unit price, it contains details on transport modes, origin and destination countries, and, critically for our analysis, identifiers for production factories and export customs ports. We geolocate each production factory and export customs port at the city level using the Amap (Gaode) API, with manual verification for any ambiguous cases.

Our primary unit of analysis is the "production factory–export customs port" pair. This pairing exhibits strong inland waterway characteristics within the Yangtze River shipping system, as most export customs ports are located in riverine port cities and navigable stretches typically exist between production factories and their corresponding ports along the Yangtze mainline or tributaries. Consequently, this route closely aligns with actual cargo flows and represents the most critical segment of the export process, as well as the segment most directly exposed to drought.

To ensure that the identified transport routes accurately reflect inland vessel movements, we implement a rigorous sample selection based on the characteristics described above. First, by matching the Industrial Enterprise Survey with the Customs Trade Statistics database, we restrict the sample to firms whose production factories and export

customs ports are both located within the Yangtze River basin. On this basis, we apply three additional screening criteria:

(1) Port attribute screening: export customs ports are required to be located in riverine port cities along the Yangtze[8] to ensure navigability along the export route.

(2) Route validity screening: to leverage the cost advantages of inland water transport over long distances and to exclude cases where drought might directly affect the production factory or port city, we retain only observations in which the production factory and export customs port are located in distinct and non-adjacent cities.

(3) Freight-relevant industry screening: given their high demand for cargo transport, we restrict the sample to firms operating in sectors with industry codes 1–43, covering agriculture, forestry, animal husbandry and fishery, mining, and manufacturing.[9]

This selection process ensures that the export paths in the sample exhibit typical inland waterway characteristics in geographic space, accurately capturing the exposure of firms to drought shocks along navigable transport channels. Our final sample comprises export information for 20,972 firms, encompassing 23,414 "production factory–export customs port" pairs. Notably, 5,074 of these firms have the capacity to export via at least two distinct shipping routes. We then calculate each firm's annual export value ($ExportValue$) along every "production factory–export customs port" shipping route and construct a panel dataset at the "firm-year-factory-port" level for the period 2000-2013.[10]

4.1.2 Climate Change Indicators

We use gridded monthly precipitation and potential evapotranspiration data from Harris *et al.* (2020) to construct the Standardized Precipitation-Evapotranspiration Index (SPEI), our primary climate indicator for drought shocks. SPEI captures the balance between water supply and atmospheric demand and is defined as:

$$SPEI_{i,t} = f\left(\sum_{k=1}^{t}(PRE_{i,k} - PET_{i,k})\right) \tag{10}$$

where $PRE_{i,k}$ denotes precipitation in region i at time k, $PET_{i,k}$ is potential evapotranspiration, and t represents the chosen time scale, typically 1, 3, 6, or 12 months. The function $f(\cdot)$ corresponds to a standardization relative to a reference climatic period. Lower values of SPEI indicate more severe drought conditions, with $SPEI < 0$ denoting

[8] Port list is based on the "China Port Code (JT/T-2002)" published by the Ministry of Transport, which specifies inland ports. The standard was issued on March 7, 2002, and implemented on May 1, 2002. We manually collected the 154 inland ports listed in this standard. https://jtst.mot.gov.cn/hb/search/stdHBDetailed?id=0f9f7f4849cf210ffe9a3087374a49ea

[9] See National Bureau of Statistics, National Economic Industry Classification (GB/T 4754-2017). https://www.stats.gov.cn/sj/tjbz/gmjjhyfl/202501/P020250116506795831658.pdf

[10] To ensure the validity of the temporal dimension, we further exclude observations in which a firm appears on a given route in only a single year.

drought and $SPEI > 0$ indicating wet conditions. We adopt the one-month SPEI as our baseline measure, as this horizon more accurately captures the immediate impact of short-term climatic anomalies on inland navigability and aligns closely with the high-frequency dynamics of firms' export decisions.

Building on the firm-year-factory-port panel constructed in subsubsection 4.1.1, we measure drought exposure along the shortest feasible inland waterway connecting each production factory to its corresponding export customs port. Since the efficiency of inland water transport depends on hydrological conditions across multiple river segments along this route, a severe drought at any single segment can create a localized disruption that constrains transport capacity along the entire route. Accordingly, we define drought exposure ($DroughtExp$) as the minimum SPEI value among all grid cells along this feasible waterway. Monthly values are aggregated to the annual level to match the yearly export data for each firm. Importantly, this measure captures route-based drought exposure, reflecting the drought constraints implied by the inland waterway network rather than the actual paths taken by firms. Formally, $DroughtExp$ is defined as follows:

$$DroughtExp_{r,y} = \text{mean}_{m\in[1,12]}\left(\min_{g\in G(r)} SPEI_{g,y,m}\right) \tag{11}$$

Here, r denotes the shortest feasible route along the inland waterway network connecting the "factory-port" pair. y denotes the year. m denotes the month within a given year, ranging from 1 to 12. $G(r)$ denotes the set of grid cells along this route. g denotes each grid cell along this route. $DroughtExp_{r,y}$ measures the drought exposure of route r in year y, defined as the annual average of the most severe drought experienced across all months m along the route. This metric captures the most vulnerable climatic conditions implied by the inland waterway network, and serves as a key variable for assessing inland waterway navigability and its impact on firms' export performance.

In practice, we manually integrate the navigable river network GIS datasets for the Yangtze River basin provided by Davis *et al.* (2025) and Yan *et al.* (2019) to identify the port city nearest to each production factory and the city corresponding to its export customs port, which serve as the origin and destination of the inland transport network, respectively. We then compute the shortest navigable path between each production factory and export customs port using a shortest-path algorithm[11] and extract the SPEI values for all grid cells along the path.

As an illustrative example, the route from Bazhong to Shanghai covers 27 prefecture-level cities, with a total river length of approximately 3,223.11 km. For each grid cell along this route, we compute monthly SPEI values and take the minimum as the drought exposure for that month (e.g., for March, June, September, and December 2000, the

[11] We employ the A* algorithm, which combines actual path costs with heuristic estimates to efficiently identify the shortest path between a start and end node in a graph.

corresponding drought exposures are -2.07, -1.04, -0.57, and -0.49, as shown in Figure 5). These monthly minima are then averaged to the annual level to characterize the most adverse climatic conditions encountered during the transport of goods from Bazhong to Shanghai via the inland waterway network.

4.2 Summary Statistics

This section reports descriptive statistics for the main variables in Table 1, providing a factual basis for the subsequent empirical analysis. The sample is organized as a panel dataset at the firm-year-factory-port level, with all monetary values expressed in thousands of RMB. To mitigate the potential influence of extreme values on the estimates, we winsorize all continuous variables at the 99th percentiles and exclude observations with anomalous zero values.

The initial sample comprises 100,177 firm-year-factory-port observations. Due to missing values in some firm-level variables, the effective sample used in the regressions is slightly smaller, but the overall proportion of missing data remains below 15 percent. Given the limited extent of missingness and the absence of systematic patterns, we consider any potential estimation bias resulting from it to be negligible for our main conclusions.

5 The Cost of Severed Links

5.1 Baseline Results

Given the large number of zero export observations and the pronounced right-skewness of the dependent variable, estimating a log-linear OLS model would not only induce sample selection concerns but could also lead to systematic distortions in coefficient estimates and their economic interpretation. As shown by Silva & Tenreyro (2006) and Cohn (2022), for trade flows and other count or nonnegative continuous outcomes, the Poisson Pseudo–Maximum Likelihood (PPML) estimator delivers consistent and robust estimates in the presence of zero-valued observations. Motivated by these methodological advantages, we estimate equation (12) using PPML. Unless otherwise noted, all subsequent empirical analyses are conducted within this PPML framework. We begin by testing Prediction 1, which posits that under infrastructure rigidity, drought shocks operate as binding capacity constraints that force a sharp contraction in export volumes (quantity rationing). Accordingly, we specify the following baseline model:

$$E(ExportValue_{i,t,r} \mid X) = \exp\left(\beta_0 + \beta_1 DroughtExp_{t,r} + \Gamma_{i,t} + \gamma_t + \delta_{i,r}\right) \tag{12}$$

Here, r denotes a factory-port route, defined as the shortest feasible path implied by the inland waterway network. $ExportValue_{i,t,r}$ denotes the export value of firm i in year t

associated with route r. $DroughtExp_{t,r}$ measures annual route-based drought exposure, defined as the minimum SPEI value across all grid cells along route r. $\Gamma_{i,t}$ is a vector of firm-level controls, including leverage (Lev), asset size ($Assets$), firm age (Age), and return on assets (ROE), which account for time-varying firm-specific characteristics. γ_t denotes year fixed effects, absorbing common shocks to exports arising from time-varying macroeconomic conditions. $\delta_{i,r}$ represents firm-route fixed effects, which control for time-invariant firm characteristics and persistent features of the geographic transport structure associated with route r. Standard errors are clustered at the firm level to account for potential serial correlation and heteroskedasticity.

Table 2 reports the baseline estimates. Consistent with the theoretical framework, we find that route-specific drought exposure acts as a severe bottleneck for trade flows. Specifically, the estimated elasticity indicates a substantial sensitivity of exports to climatic capacity constraints. As detailed in Column (2), a one-standard-deviation intensification in drought severity (corresponding to a decrease in $DroughtExp$) precipitates an approximately 22 percent contraction in export value along the affected route.[12] This result is not only statistically significant but also economically meaningful, indicating that climate-induced drought constrains inland waterway transport capacity and generates a substantial adverse impact on firms' exports.

To further examine heterogeneity in the effects across different drought severity levels, we discretize the continuous route-level drought exposure measure ($DroughtExp$) into five intervals based on the 20th, 40th, 60th, and 80th percentiles of its distribution. We then construct a set of indicator variables, D_q, where $D_q = 1$ if the drought exposure of route r in year t falls within percentile bin q, and $D_q = 0$ otherwise. The corresponding empirical specification is given by:

$$E(ExportValue_{i,t,r} \mid X) = \exp\left(\beta_0 + \sum_{q=1}^{5} \beta_q D_q + \Gamma_{i,t} + \gamma_t + \delta_{i,r}\right) \tag{13}$$

Here, β_q captures the differential response of exports to drought exposure across intensity bins. The estimates reported in Figure 6 show that, relative to routes in the least drought-exposed group (the 80–100 percentile bin), routes facing extreme drought exposure (the 0-20 percentile bin) experience the largest reduction in exports. The magnitude of this decline under extreme drought substantially exceeds that observed under moderate or mild drought exposure, indicating a pronounced nonlinearity in the export response and an amplification of drought impacts at the severe end of the exposure distribution.

[12] Within the PPML framework, the economic magnitude is evaluated via the exponential transformation $\exp(\beta\Delta x) - 1$. Given the estimated coefficient $\hat{\beta}_1 = 0.5902$ and the standard deviation of the drought index ($\Delta x \approx 0.33$), the average impact is calculated as $\exp(0.5902 \times 0.33) - 1 \approx 22\%$. This magnitude represents the average percentage divergence in export volumes relative to the counterfactual scenario of normal hydrological conditions.

5.2 Robustness

We assess the robustness of the baseline findings through a comprehensive set of checks that vary the construction of key variables, alter sample selection criteria, implement placebo tests, and account for potential confounding factors.

(1) Alternative Port Identification Criteria. To ensure consistency in route and port identification, the baseline specification constructs port nodes and the inland shipping network based on the *China Port Codes (JT/T-2002)*. However, because the Ministry of Transport does not publish annual updates on newly established ports, the 2002 port list may undercount inland ports added in later years, potentially introducing geographic matching error and sample selection bias. To address this concern, we re-identify port nodes using the revised *China Port Codes (JT/T-2015)* issued by the Ministry of Transport.[13] Using this updated port list, we reconstruct the set of feasible inland port nodes that can serve as potential shipping origins for each production factory, and update the corresponding factory-port matches and shipping routes accordingly. The resulting regression estimates are reported in Table A1. The coefficient on the key explanatory variable remains stable in both sign and statistical significance, indicating that the baseline findings are not driven by port identification error.

(2) Alternative Measures of Drought Exposure. To examine whether our results are sensitive to the specific construction of drought measure, we construct six alternative drought exposure indicators. Table A2 reports the corresponding estimation results under these alternative specifications. Among these measures, $DroughtExpWeighted_{avg01}$ and $DroughtExpWeighted_{min01}$ extend the baseline indicator by incorporating weights based on waterway class, reflecting the idea that navigational sensitivity to drought varies systematically with channel width. Intuitively, narrower waterways are more likely to experience binding navigability constraints under drought conditions. Following the *Inland Waterway Navigation Standards (GB 50139–2014)* issued by the Ministry of Transport,[14] we first assign a waterway class to each grid cell, defined as the class of the longest navigable segment within that cell (see Figure A1). We then incorporate these class-based

[13] The JT/T-2015 standard was released on April 24, 2015, and implemented on July 31, 2015, on which date the JT/T-2002 standard was repealed. We manually compiled the list of inland ports specified in the revised standard, yielding a total of 183 inland ports—29 more than the 154 inland ports included in the 2002 version. https://jtst.mot.gov.cn/hb/search/stdHBDetailed?id=f816cfe700d02af618aae5e6b6729221

[14] The standard was released on April 15, 2014, and implemented on January 1, 2015. The maximum allowable vessel convoy widths (two-way, in meters) for Class I to Class V waterways are 250, 190, 110, 90, and 70, respectively. http://cqfz.wti.ac.cn/wti/dbfile.svl?n=/u/cms/www/202103/121359 5519ma.pdf

weights into the construction of drought exposure as follows:

$$DroughtExpWeighted_{r,y} = \text{mean}_{m\in[1,12]}\left[\min(\text{or mean})_{g\in G(r)} w_{l(g)} \times SPEI_{g,y,m}\right] \tag{14}$$

$$w_{l(g)} = \frac{MaxWidth_5}{MaxWidth_{l(g)}} \tag{15}$$

where r denotes the shortest feasible route along the inland waterway network connecting the "factory-port" pair. y denotes the year. m denotes the month within a given year, ranging from 1 to 12. $G(r)$ denotes the set of grid cells along this route. g denotes each grid cell along this route. $w_{l(g)}$ denotes the weight assigned to grid cell g, and $l(g)$ indicates its waterway class. The weight is defined as the ratio of the maximum allowable width of a Class 5 waterway to that of class $l(g)$. $DroughtExpWeighted_{r,y}$ denotes the route-level drought exposure measure that accounts for heterogeneity in waterway class.

In addition, we construct several alternative measures of route-based drought exposure to examine the sensitivity to different temporal scales. First, $DroughtExp_{avg01}$ replaces the baseline minimum-SPEI metric with the average 1-month SPEI across all grid cells along the route. We also compute $DroughtExp_{min03}$, $DroughtExp_{min06}$, and $DroughtExp_{min12}$, corresponding to the minimum SPEI along the route computed at 3-, 6-, and 12-month accumulation periods, respectively, by adjusting the time scale parameter t in Equation 10. The results indicate that among these six alternative measures, only the 12-month accumulated drought exposure ($DroughtExp_{min12}$) is statistically insignificant, suggesting that long-term drought has limited effects on firms' short-term export decisions. Overall, introducing waterway class weights and alternative temporal scales does not alter the sign or significance of the core route-based drought exposure variable.

(3) Alternative Route Length Criteria. To mitigate the direct influence of drought in the cities hosting production factories or export customs ports, the baseline sample includes only routes for which the factory and port are non-adjacent, defined as "firm–route" observations with more than two intermediate cities along the route. Building on this, we vary the threshold for the number of intermediate cities to greater than 1, 3, and 4, respectively, to examine the sensitivity of our results to this sample selection criterion. The estimates reported in Table A3 indicate that the coefficient on the key route-based drought exposure variable remains stable in both sign and statistical significance across these alternative specifications. This suggests that the baseline findings are not driven by a particular route length or route structure.

(4) Placebo Test in the Yellow River Basin. To validate the exclusion restriction underlying our identification strategy, we implement a falsification test in the Yellow River Basin. This region serves as an ideal counterfactual: while it shares similar macroclimatic patterns with the Yangtze, it lacks a commercially navigable inland waterway

network, thereby structurally shutting down the transport transmission channel. We strictly replicate the baseline sample construction and estimation procedures for this control group.

The results, reported in Table A4, yield a coefficient that is statistically indistinguishable from zero. Crucially, the drastic reduction in sample size—yielding only 571 valid observations compared to the vast Yangtze sample—is not a data limitation but a structural feature. It mechanically reflects the absence of the specific factor (navigable waterways) in this region. This null result provides compelling evidence that our baseline estimates isolate the specific mechanism of inland shipping connectivity, effectively ruling out spurious correlations driven by general regional productivity shocks or unobserved macro-climatic trends.

(5) Controlling for Alternative Climate Channels To further address potential confounding factors, we consider additional climate variables that may simultaneously affect route-level exports and drought exposure. Since inland waterway navigability largely depends on upstream inflows, we augment the baseline specification with: (i) the average drought indicator across grid cells covering the upstream river network corresponding to each route ($DroughtExp_{upstream}$), (ii) upstream runoff ($Upflow$), and (iii) drought exposure at the production factory location ($DroughtExp_{industry}$).[15] The results, reported in Table 3, show that after including these additional controls, the coefficient on the key route-based drought exposure variable remains stable in both sign and statistical significance. This indicates that the negative effect of drought on firm exports primarily operates through constraints on inland waterway transport, rather than local or upstream climatic conditions at the production site.

5.3 Quantity Rationing at the Intensive Margin

we isolate the physical locus of the export contraction. If drought indeed functions as a binding capacity constraint rather than a linear cost shock, we should observe a sharp reduction in the intensive margin of trade—specifically, the effective load factor of transport vessels. To test this, we expand our baseline panel to the product dimension and construct two granular metrics: $Goods_{num}$, the total export volume of a specific product on a given route; and $Goods_{avg}$, the average quantity per customs transaction. As noted in the institutional background, the latter serves as a proxy for the average cargo load per vessel, given the "one-batch-one-vessel" nature of inland customs declarations .[16]

The results, reported in Table A5, provide direct evidence of physical rationing. We find that intensified drought exposure precipitates a significant collapse in both total

[15] Runoff data are sourced from Abatzoglou *et al.* (2018).

[16] Under China's customs declaration system, exports are typically reported on a batch basis, and a single customs record rarely corresponds to multiple vessels.

export volumes and, crucially, the average shipment size ($Goods_{avg}$). This contraction at the intensive margin confirms the "light-loading" mechanism: as navigable depth decreases, vessels are physically compelled to reduce their draft by carrying less cargo per voyage to avoid grounding.

5.4 Price Rigidity

To comprehensively characterize the market clearing mechanism, we examine the response of export unit values. Standard trade theory suggests that if demand is inelastic, supply shocks should trigger price surges. However, under the Small Open Economy assumption, firms are price-takers in global markets. In this scenario, the "shadow cost of congestion" (λ) identified in our model creates a wedge that cannot be passed through to consumers, forcing adjustment entirely through quantity rationing.

We test this hypothesis using a firm-goods-year panel to estimate changes in export unit prices. The results, reported in Table A6, reveal a striking price rigidity: under higher route-based drought exposure, export prices remain statistically unresponsive. This null result confirms that the logistical friction does not manifest as a mark-up in the transaction price. Instead, it operates as an internal shadow cost wedge—comprising delays, uncertainty premiums, and coordination efforts—that absorbs firm margins.

This combination—sticky prices and collapsing volumes—validates the quantity rationing mechanism. Given the high price elasticity of international buyers, firms face a rigid demand curve. When drought-induced capacity constraints drive the effective transport cost (explicit freight implicit shadow cost) above the transaction's break-even point, the rational equilibrium is not price renegotiation, but volume destruction (e.g., order cancellations or shipment postponements). Anecdotal evidence corroborates this "rationing" behavior. For instance, during shipping capacity crunches, international buyers frequently refuse to absorb freight surcharges, forcing exporters to suspend shipments entirely to "wait and see."[17] Thus, the market clears through a logistical squeeze that crowds out trade quantities, rather than through price signals.

6 Mechanism: Unpacking the Shadow Cost of Congestion

Having established the aggregate quantity rationing effect, we now turn to Prediction 2 (Propagation of Shadow Costs). Our theoretical framework posits that under infrastructure rigidity, the binding capacity constraint generates a positive shadow price of congestion ($\lambda > 0$). While this shadow cost is implicit, it must manifest empirically

[17] See, for example, reports from the Zhejiang Provincial Government indicating that when container freight rates from Ningbo to South America surged from $3,000 to $8,000, international clients refused to bear the cost, leading to widespread shipment delays. Available at: https://zcom.zj.gov.cn/art/2024/6/28/art_1384592_58945100.html.

through tangible frictions. In this section, we verify this propagation along three distinct layers: (1) the physical layer, where hydrological anomalies degrade shipping efficiency; (2) the accounting layer, where implicit frictions materialize into explicit operating costs; and (3) the financial layer, where credit constraints act as an amplifier of the real shock.

In the Yangtze River basin, drought shocks primarily operate through tightened and disrupted inland shipping conditions. Prolonged drought lowers river water levels, thereby constraining channel navigability, reducing allowable vessel draft, lengthening transit times, and intermittently creating shortages in shipping capacity. These disruptions raise transportation costs and increase delivery uncertainty, directly weakening firms' ability to fulfill export contracts and potentially disrupting production organization and export timing.

Beyond these direct effects, impaired inland shipping can further amplify export contractions through multiple channels, including higher operating costs, tighter financing constraints, and production inefficiencies arising from supply–demand mismatches.

Building on the above logic, this section conducts a systematic examination along three dimensions: (1) Shipping conditions: whether drought reduces transportation efficiency by lowering water levels and constraining vessel navigability; (2) Costs: whether disruptions to inland shipping significantly increase firms' transportation and export costs; and (3) Financing: whether cash-flow pressures induced by higher logistics costs and greater delivery uncertainty further suppress firms' export investment and expansion.

6.1 Shipping condition

6.1.1 Drought and water level

We first examine whether drought affects inland transport efficiency by altering shipping conditions. Water levels constitute the key physical constraint on navigability, directly determining vessel draft, cargo capacity, and transit safety, and thereby shaping the stability and economic performance of the shipping system. High water levels allow larger vessels to navigate smoothly, supporting efficient transport and uninterrupted supply chains. In contrast, substantial declines in water levels reduce channel depth, increase the risk of grounding, and may even lead to temporary closures of critical river segments. The resulting reductions in shipping capacity and delays are the primary physical channel through which drought shocks affect inland regions' export.

To examine this mechanism, we use water level data published by the National Large River Real-Time Hydrological Monitoring Center of the Ministry of Water Resources, covering major hydrological stations from July 2021 to December 2023. We construct a panel dataset at the station-year-month level, using the water level recorded on the last day of each month as the observation. For each station, we match the $SPEI$ of the corresponding grid cell as a measure of drought exposure, which allows us to estimate

the effect of drought on river water levels. The results, reported in Table A7, indicate that a one-standard-deviation increase in drought exposure (i.e., a one-standard-deviation decline in $SPEI$) is associated with an average water level decline of approximately 0.2 meters at the station. This evidence directly confirms that drought reduces navigable water levels and shipping capacity.

6.1.2 Drought and vessel status

To further explore the transmission of drought through shipping channels to firm exports, we use vessel-level data from the global Automatic Identification System (AIS).[18] The dataset records the position of each vessel at a near-second-level frequency and covers the period from 2021 to 2022. We select cargo vessels operating within the Yangtze River basin based on vessel type and, on this basis, perform data cleaning and route identification.

Given the massive volume of near-second-level AIS data, we implement preprocessing.[19] The processed vessel trajectories are then converted into binary time-series movement vectors, where "0" indicates a stationary (docked) state and "1" indicates a sailing state. This sequence can be interpreted as a discrete state-transition process over time. To reduce noise caused by instantaneous positioning errors or short-term speed fluctuations, we apply a sliding-window smoothing procedure to the state sequence, eliminating spurious state changes. Consecutive segments of "1" are defined as a single effective voyage, representing uninterrupted sailing from departure to the next docking. We further screen voyages for spatiotemporal consistency.[20] To ensure geographic comparability with our firm-level export panel, we retain only voyages whose origin and destination cities are separated by at least one intermediate city.

We calculate two core measures for each vessel: port stay duration ($StayDuration$) and voyage duration ($VoyageDuration$). These measures are matched with the $DroughtExp$ value corresponding to the departure month of the voyage, capturing the drought exposure faced by the vessel. Notably, port stay duration is matched with the lagged $DroughtExp$ to capture vessel behavioral responses to prior drought exposure. The corresponding panel descriptive statistics are reported in Table A8, with all continuous variables winsorized at the 99th percentiles.

The empirical results are reported in Table 4. The estimates show that an increase

[18] Data are provided by the China Economic Information Service (CEIS).

[19] Specifically, we first aggregate the second-level positional data to the hourly level and use the Haversine formula to calculate the distance between consecutive observations, thereby characterizing vessel movement within each hour. Next, combining port coordinates from the China Port Code (JT/T-2002) and vessel speed, we classify observations as "in port" if the speed is below 2.5 knots and the vessel is within 50 nautical miles of the nearest port; all other observations are defined as "underway."

[20] Specifically, we exclude observations with anomalous time gaps, implausibly large spatial jumps, or docking durations that deviate substantially from the sample mean.

in drought exposure significantly prolongs vessels' port stay duration, indicating that droughts compress navigable water levels and induce vessels to wait longer for favorable sailing windows. By contrast, vessels experience extended voyage duration during the transit phase under drought exposure, manifesting as a significant downward adjustment in speed.

To further examine heterogeneity across vessel types, we split the sample at the median vessel length of 58.7 meters into large- and small-vessel groups and estimate the models separately.[21] The results show that, under intensified drought exposure, large vessels experience a significant increase in port stay duration and a reduction in average sailing speed during voyages. This pattern is consistent with their deeper draft and greater sensitivity to water-level fluctuations, reinforcing the interpretation that droughts impair inland shipping capacity through physical navigability constraints.

6.2 Firm Expenditures

This subsection further examines whether route-based drought exposure translates into higher costs at the firm level. We construct a firm-year panel as the primary unit of analysis. For firms associated with multiple factory-port pairs in a given year, we compute the average route-based drought exposure across all corresponding routes to obtain a firm-level measure of overall exposure to drought-induced inland waterway constraints. Descriptive statistics for the resulting panel are reported in Table A9.

$$E\big(Spending_{i,t} \mid X\big) = \exp\Big(\beta_0 + \beta_1 DroughtExp_{i,t} + \Gamma_{i,t} + \gamma_i + \delta_t\Big) \tag{16}$$

where $Spending_{i,t}$ denotes expenditure measures for firm i in year t, including cost of sales and administrative expenses; $\Gamma_{i,t}$ denotes a series of control variables; and γ_i and δ_t denote firm and year fixed effects, respectively.

To examine how drought shocks affect firms' cost structure through disruptions in inland shipping, we focus on two key financial ratios: the cost of sales ratio

$$CostRatio = \frac{Sales\ Costs}{Industrial\ Sales}$$

and the overhead ratio

$$OverheadRatio = \frac{Overheads}{Industrial\ Sales}$$

The underlying mechanism is as follows. When drought reduces water levels along critical shipping routes, firms face delays in raw material delivery, higher alternative

[21] According to the Standard Dimensions of Inland Lock-Transiting Vessels, Part I: Yangtze River System (GB 38030.1–2019), cargo vessels operating on the Yangtze mainline typically range from 88 to 130 meters in length, indicating that most fall into the large-vessel category.

logistics costs, and additional operational challenges. These pressures are reflected in an increase in *CostRatio*, capturing elevated direct production and transportation costs, and in an increase in *OverheadRatio*, capturing indirect management and risk mitigation expenses. The latter includes costs associated with contract risk management (e.g., order delays or performance guarantees), emergency logistics adjustments (e.g., temporary storage, rerouting via road or multimodal transport), and supply chain financing pressures arising from extended delivery times and delayed payments.

The estimates reported in Table 5 confirm these mechanisms: higher drought exposure along firms' shipping routes is associated with significant increases in both *CostRatio* and *OverheadRatio*. These results indicate that drought not only directly raises transportation costs through reduced navigable water levels but also amplifies broader operational burdens via multiple indirect channels.

6.3 Financial Constraints

The preceding empirical results show that droughts impose operating pressure on firms by constraining shipping capacity and raising transportation costs. In this context, when firms face limited access to external finance and are unable to smooth liquidity shocks, the adverse effects of drought are more likely to be amplified, resulting in a stronger negative impact on firms' exports. This subsection examines heterogeneity in the effects of drought shocks across firms with differing degrees of financing constraints.

We measure firms' financing constraints using the SA index (Size-Age Index) proposed by Hadlock & Pierce (2010), which is computed as follows:

$$SA_{i,t} = -0.737 \times \text{Size}_{i,t} + 0.043 \times \text{Size}_{i,t}^2 - 0.040 \times \text{Age}_{i,t}, \tag{17}$$

where $\text{Size}_{i,t}$ denotes the asset size of firm i in year t (measured as the natural logarithm of total assets), and $\text{Age}_{i,t}$ captures firm age. Values of the index closer to zero are typically interpreted as indicating tighter financing constraints; in our sample, larger values of the SA index correspond to more severe financing constraints faced by firms.

We introduce an interaction term between firm-level route-based drought exposure and financing constraints in the panel data to identify the amplifying role of financing constraints in transmitting drought shocks. The empirical specification is given by:

$$\begin{aligned} E\big(ExportValue_{i,t} \mid X\big) = \exp\Big(&\beta_0 + \beta_1 DroughtExp_{i,t} \times SA_{i,t} \\ &+ \beta_2 DroughtExp_{i,t} + \beta_3 SA_{i,t} + \Gamma_{i,t} + \gamma_t + \delta_i\Big) \end{aligned} \tag{18}$$

Table 6 reports the corresponding estimation results. The coefficient on the interaction term is positive and statistically significant, indicating that financing constraints materially amplify the negative impact of drought shocks on firm exports.

Overall, the empirical evidence in this section elucidates the anatomy of the transmission mechanism. We show that hydrological droughts act as a fundamental productivity shock that degrades the physical efficiency of the specific factor—inland waterways—thereby translating implicit navigational frictions into explicit operating costs. For financially constrained firms, this transmission is non-linear and catastrophic. These agents face a "double shock": the first is the physical quantity rationing that mechanically severs market access, and the second is the financial accelerator that amplifies the economic damage due to an inability to smooth the resulting liquidity drain. Thus, the magnitude of the trade collapse is jointly determined by the interaction between infrastructure rigidity and financial fragility.

7 Infrastructure Lock-in and Second-Best Adjustments

Having documented the surge in shadow costs and the resulting quantity rationing, we now examine firm-level adaptation strategies. Standard trade theory predicts that when the cost of one transport mode spikes, rational agents should arbitrage the price wedge by substituting towards alternative modes (e.g., rail or road). However, our Prediction 3 (Infrastructure Lock-in) posits that for bulk commodities dependent on inland waterways, such substitution entails prohibitive switching costs, rendering the transport network rigid in the short run.

In this section, we test this rigidity hypothesis and explore the consequent second-best adjustments. We show that because firms are physically "locked in" to the waterway network, they cannot smooth the shock through logistical diversification. Instead, they are forced to reallocate resources across margins where they retain flexibility: substituting intertemporally via inventory accumulation and spatially by shifting sales to domestic markets.

7.1 Intermodal Substitution

To empirically test the degree of infrastructure rigidity, we first assess whether firms can mitigate drought shocks by switching to the railway or highway network. If intermodal substitution is frictionless, firms in industries with higher technological substitutability should experience smaller export declines.

We quantify the potential for substitution using two industry-level proxies, $SwitchToRailway$ and $SwitchToHighway$. Leveraging the 1997 Input-Output Tables, we construct a "substitution index" based on the technological production function of each industry. Specifically, the railway substitution index is defined as the difference between an industry's

reliance on rail versus water transport, normalized by its total logistics intensity:

$$SwitchToRailway_i = \frac{IO_{i,rail} - IO_{i,water}}{IO_{i,water} + IO_{i,road} + IO_{i,rail} + IO_{i,air} + IO_{i,pipe} + IO_{i,other}} \quad (19)$$

where $SwitchToRailway_i$ measures the substitutability of rail for water transport in industry i. $IO_{i,water}$ is the intermediate input from the water transport sector, scaled by the industry's total transport inputs across six modes. Theoretically, greater substitution possibilities imply a higher elasticity of mode switching, which should mitigate the negative impact of droughts on export performance. The highway index ($SwitchToHighway$) is defined similarly.

The estimates, reported in Table 7, provide strong empirical support for Prediction 3. The coefficients on the interaction terms ($SwitchToRailway \times DroughtExp$ and $SwitchToHighway \times DroughtExp$) are consistently statistically insignificant or economically negligible. This "null result" is structurally meaningful: it implies that even for industries where intermodal substitution is technologically feasible (as indicated by I-O tables), it remains economically prohibitive in the short run. This result points to substantial adjustment costs, driven by capacity limits and scheduling rigidities in rail and road networks, which hinder the short-term reoptimization of supply chains.

7.2 Structural Determinants of Transmission

Given the modal lock-in established above, our framework suggests that the magnitude of the export contraction should depend on two structural parameters: the firm's reliance on the specific factor (α) and the time sensitivity of its goods (which determines the shadow cost λ). We test these heterogeneous effects to further identify the transmission mechanism.

Variation in Waterway Dependence. We first examine whether the extent to which firms rely on inland waterway transport affects the transmission of drought shocks. To this end, we construct a firm-level waterway dependence index ($WaterwayDep$) using the industry-level input-output table, which proxies for the firm's dependence on inland waterway transport. Specifically, we use the 1997 input-output table for 124 Chinese sectors to calculate, for each industry, the share of "inland waterway transport" in total transportation services inputs. Formally, this is defined as:

$$WaterwayDep_i = \frac{IO_{i,water}}{IO_{i,water} + IO_{i,road} + IO_{i,rail} + IO_{i,air} + IO_{i,pipe} + IO_{i,other}} \quad (20)$$

where $IO_{i,water}$ denotes the intermediate input of industry i in inland waterway transport, and the denominator is the industry's total intermediate inputs across six modes of transportation.

This index reflects the relative dependence of industry production activities on inland waterway transport. Industries with high waterway dependence typically produce bulk commodities that are low in unit value and relatively insensitive to delivery speed, such as nonferrous metal mining and processing, and petroleum and coal processing. In contrast, industries producing higher-value goods with greater requirements for flexibility and timeliness—such as chemical fiber manufacturing, pharmaceuticals, and precision instruments—tend to rely more on road or air transport.

To validate the measure, we manually classify industries according to the *National Economic Industry Classification (GB/T 4754–2017)* into three groups: heavy industry (mining, smelting, petroleum, and large-scale processing), light industry (food, textiles, furniture, etc.), and high-technology manufacturing (electronics, pharmaceuticals, instruments). Descriptive statistics for these groups are presented in Figure A2. Heavy industry exhibits substantially higher waterway dependence at the industry level compared with the other two groups. This pattern is consistent with the bulk commodity characteristics and low unit value of its products, suggesting that the index captures the alignment between product characteristics and transport mode choice. Further, a cross-industry nonparametric comparison using the Kruskal-Wallis test rejects the null hypothesis of identical distributions of waterway dependence across heavy, light, and high-technology industries (p-value = 0.0571), which aligns with economic intuition.

Building on this measure, we classify firms into a high waterway dependence group ($WaterwayDep = 1$) and a low waterway dependence group ($WaterwayDep = 0$) based on the median of the industry-level distribution. To examine whether the impact of route-based drought exposure differs across firms with varying dependence, we introduce an interaction term between drought exposure and the waterway dependence indicator into the baseline specification. The model is formally specified as follows:

$$E\big(ExportValue_{i,t,r} \mid X\big) = \exp\Big(\beta_0 + \beta_1\, DroughtExp_{r,t} \times WaterwayDep_i + \beta_2\, DroughtExp_{r,t} + \beta_3\, WaterwayDep_i + \Gamma_{i,t} + \gamma_t + \delta_{i,r}\Big) \quad (21)$$

Columns (1)–(2) of Table 8 report the corresponding estimates. Column (2) shows that the coefficient on the interaction term is positive and statistically significant at the 10% level, indicating that, compared with firms with low waterway dependence, droughts have a stronger suppressive effect on exports for firms that rely more heavily on waterway transport. Although the level of significance is modest—likely because the initial sample selection already largely isolates firms whose exports depend on inland waterways, so further splitting by waterway dependence within this already waterway-reliant sample reduces the identifiable variation—the result nonetheless supports our core mechanism: the negative impact of drought on exports is concentrated among firms whose transportation needs are highly reliant on waterways, confirms that the bindingness of the

capacity constraint is strictly increasing in the firm's reliance on the waterway network.

Variation in Time Sensitivity. Second, we test whether the impact varies with the time sensitivity of goods. Theoretically, for products with short shelf lives or high customization (high time sensitivity), the shadow cost of delay is prohibitive, as inventory accumulation is not a viable buffer.

To characterize the time sensitivity of goods, we leverage industry-level information on each firm's primary business and apply the DeepSeek v3.1 large language model to semantically classify industry descriptions. Specifically, based on production processes and product characteristics, firms are grouped into high time sensitivity ($TimeSensitivity = 1$) and low time sensitivity ($TimeSensitivity = 0$). The model parameters and classification criteria are reported in Figure A3 and Figure A4.

The classification evaluates industry characteristics along five dimensions: product perishability and seasonality, production cycle length, inventory features, trade organization, and market adaptability. High time sensitivity industries generally produce goods with short shelf lives or strong seasonality, long and customized production cycles, high-cost and easily perishable inventories, reliance on long-term contracts or specialized equipment, and relatively rigid market use with high customer switching costs. In contrast, low time sensitivity industries tend to feature standardized production, lower inventory costs, and greater market flexibility.

To assess robustness, we randomly selected 20 firms and repeated the classification 20 times for each. Nineteen firms were consistently classified across repetitions, indicating that the LLM-based method provides stable and reproducible time sensitivity assignments (see Figure A5).

Building on this classification, we further examine the interaction between drought exposure and time sensitivity of goods. The corresponding model is specified as follows:

$$E\big(ExportValue_{i,t,r} \mid X\big) = \exp\Big(\beta_0 + \beta_1\, DroughtExp_{r,t} \times TimeSensitivity_i + \beta_2\, DroughtExp_{r,t} + \beta_3\, TimeSensitivity_i + \Gamma_{i,t} + \gamma_t + \delta_{i,r}\Big) \quad (22)$$

Columns (3)-(4) of Table 8 report the corresponding estimates. The interaction term is positive and statistically significant, indicating that route-based drought exposure has a stronger negative effect on exports of firms producing highly time-sensitive goods. This finding aligns closely with theoretical expectations: for time-sensitive products, shipping delays increase the risk of order defaults, inventory losses, and market share erosion, and droughts amplify these risks by constraining inland waterway transport. In contrast, firms with less time-sensitive products can more readily mitigate adverse impacts through delayed shipments or increased inventory.

7.3 Second-Best Adjustments: Inefficiency and Trade Diversion

With the first-best solution—intermodal substitution—rendered inaccessible by infrastructure rigidity, firms must resort to second-best adjustments to manage the capacity rationing. We conceptualize these responses as a constrained optimization problem where agents reallocate resources across three remaining accessible margins: intertemporal, spatial, and market-based. We examine the efficacy of these strategies in dampening the drought-induced export decline.

(1)Production and Operational Adjustments. Theoretical models suggest that firms can smooth supply shocks either by adjusting production plans or by utilizing inventories. However, given the rigidity of production schedules in the short run, we hypothesize that the primary margin of adjustment is inventory accumulation. This strategy acts as an intertemporal buffer, allowing firms to stockpile output during logistical bottlenecks to prevent immediate supply chain rupture, albeit at the cost of higher working capital requirements.

(2)Transport and Supply Chain Reconfiguration. While firms cannot switch transport modes (e.g., water to rail), they retain some flexibility to optimize routes within the waterway network. We examine whether firms engage in spatial arbitrage by shifting export clearance to alternative customs ports with lower drought exposure. This "route switching" represents a search for residual capacity within a constrained network .

(3)Market Diversion. When access to international markets is severed, firms must find alternative vents for surplus output to satisfy their budget constraints. We investigate trade diversion, testing whether firms substitute blocked export sales with domestic sales (q_d). This reallocation serves as a revenue hedge, ensuring cash flow continuity even as foreign market access collapses.

In the empirical analysis that follows, we dissect these three margins to identify the micro-foundations of firm resilience. We aim to determine which of these second-best strategies effectively buffers the climate shock and how their efficacy varies with firm-level constraints, such as goods time sensitivity and waterway dependence.

7.3.1 Production and Operational Adjustments

Firms primarily respond to drought shocks by adjusting production and inventory to smooth logistical and market volatility. We isolate these responses using a triple interaction approach within a firm-level panel framework. We estimate the following

equation:

$$E\big(Production_{i,t} \text{ or } Inventory_{i,t} \mid X\big) = \exp\Big(\beta_0 + \beta_1 DroughtExp_{i,t} \times WaterwayDep_i \times TimeSensitivity_i + \Gamma_{i,t} + \gamma_t + \delta_i\Big) \tag{23}$$

Where $Production_{i,t}$ is the production intensity of firm i in year t, proxied by the ratio of industrial output to sales; $Inventory_{i,t}$ measures inventory levels using the ratio of total (or finished goods) inventory to sales; and $DroughtExp_{i,t}$ is the route-weighted average drought exposure faced by the firm. The terms γ_t and δ_i are year and firm fixed effects.

Table 9 investigates the impact of drought-induced shipping constraints on production. We find no statistically significant relationship between drought exposure and production levels. Similarly, we observe no significant heterogeneity when splitting the sample by shipping dependence or product time-sensitivity. These null results imply that the direct impact of climate shocks on firm production is minimal.

We attribute this null result to the planned nature of production. Constrained by fixed capacity and contracts, production is less agile than downstream activities like shipping. To verify this, we estimate specifications including 1-year and 2-year lags of drought exposure. The results in Table A10 show no significant lagged effects, confirming that production output remains unresponsive to drought shocks even over longer horizons.

In sharp contrast, firms exhibit significantly greater flexibility in inventory management. Table 10 presents the estimation results, where Columns (1)–(3) and (4)–(6) employ total inventory ($Inventory/IndustrialSales$) and finished goods inventory ($FinishedGoods/IndustrialSales$) as proxies, respectively. We find that elevated drought exposure leads to a statistically significant increase in both total and finished goods inventories, an effect that is particularly pronounced for firms with high shipping dependence. This suggests that firms stockpile inventory to hedge against logistical risks amidst shipping constraints and delivery uncertainty. However, for firms producing time-sensitive goods, the triple interaction coefficient is significantly negative, indicating constrained scope for inventory adjustment. Due to short shelf lives or strict timeliness requirements, these firms cannot rely on inventory accumulation to buffer disruptions and must instead resort to alternative adaptive strategies to maintain supply continuity.

Overall, drought shocks leave production levels largely unchanged but trigger significant inventory responses. While inventory buildup acts as an effective hedge for firms with low time-sensitivity, its role is restricted for time-sensitive products. For the latter group, the locus of adaptation likely shifts away from inventory management toward the optimization of transportation modes and alternative market channels.

7.3.2 Transport and Supply Chain Reconfiguration.

Cross-Factory Production Shifting. Firms may also reconfigure production internally. Using customs data to identify factory locations, we build a firm-year-factory dataset. We define a differential shock variable, $DroughtExp_{other}$, calculated as the drought exposure of the firm's other factories minus that of the focal factory. This captures the incentive to shift production. Theoretically, if firms substitute away from high-risk locations, higher exposure at other factories should correspond to increased export activity at the focal factory.

Table 11 confirms that firms shift production toward less exposed factories: focal factory exports rise when other factories face higher drought exposure. We find no significant heterogeneity in this effect. However, the scope of this mechanism is limited. The identification relies on a restricted sample of 339 multi-factory firms(4,493 observations), significantly fewer than the 19,703 baseline firms. This indicates that most firms are single-factory producers. Therefore, intra-firm reallocation is constrained by production layout and scale, preventing it from acting as a widespread buffer against climate shocks.

Route Switching. Comparatively, adjustments at the route level are substantial. We employ a firm-year-route panel to identify port switching, defining $DroughtExp_{other}$ as the exposure gap between alternative export ports and the focal port for the same factory. The sample includes 4,912 firms and 35,496 observations—those with multiple route options. Unlike the factory-level analysis, this sample offers high representativeness and captures a widespread adaptive behavior.

Table 12 shows that firms shift exports to routes that are less exposed to drought than their alternatives. This reallocation is stronger for shipping-reliant firms but does not vary by time-sensitivity. Since the Yangtze offers few alternative water paths, this finding implies that firms manage risk by switching customs ports to shorten the duration of river transport. By reducing the reliance on long-distance water haulage, firms likely substitute the vulnerable water segment with alternative transport modes.

To comprehensively assess the relative importance of adjustments made by enterprises at different levels, we further compared the benchmark regression results at the enterprise level, factory level and route level. Table A11 shows that a one-standard-deviation worsening of drought conditions reduces exports by roughly 14.4% (firm), 15.4% (factory), and 20.8% (route). The significantly larger impact at the route level points to route and port selection as the principal adjustment channel. The similarity of firm- and factory-level coefficients confirms that spatial production shifting plays a minor role for the typical firm.

To conclude, supply chain adjustments are stratified by feasibility. With mode switching and factory relocation limited by rigid constraints, inter-route shifting stands out as the most viable response. This is especially true for shipping-intensive firms,

for whom port reconfiguration acts as a vital buffer. Ultimately, our evidence suggests that firms weather drought shocks primarily through the malleability of their logistics networks, not by fundamentally changing where they produce.

7.3.3 Market Diversion

In addition to operational changes, firms can adapt by restructuring their market layouts to ensure business continuity. We focus here on two longer-term strategies: shifting sales toward the domestic market and diversifying the export portfolio.

First, we test if firms substitute foreign sales with domestic sales in response to drought shocks. We quantify this shift using a domestic sales share metric, constructed from the firm-level panel as follows:

$$DomesticShare_{i,t} = 1 - \frac{ExportValue_{i,t}}{IndustrialSales_{i,t}} \tag{24}$$

where $IndustrialSales_{i,t}$ is the total industrial sales of firm i in year t.

Table 13 shows that drought intensification significantly increases the domestic sales share (Column 1), as indicated by the negative coefficient. This points to an export-to-domestic substitution strategy to buffer external shocks. While this pattern is consistent across varying levels of shipping dependence, it is significantly stronger for time-sensitive goods (Column 3). High time-sensitivity implies high storage costs and delivery urgency; thus, these firms preferentially channel output to the domestic market to avoid inventory backlogs and delivery failures.

We further test whether firms mitigate shocks through export diversification. The model, estimated using route-level panel data, is given by:

$$E(Diversity_{i,t,r} \mid X) = \exp\left(\beta_0 + \beta_1 DroughtExp_{t,r} + \Gamma_{i,t} + \gamma_t + \delta_{i,r}\right) \tag{25}$$

where $Diversity_{i,r,t}$ captures export diversification for firm i along route r in year t. We proxy for this diversity using the count of destination countries ($Export_{CountryType}$) and the number of distinct product types ($Export_{GoodsType}$).

As shown in Table A12, drought shocks negatively impact export variety at the route level but show no significant effect at the firm level. This implies that firms do not shrink their overall product offerings but rather reallocate exports across shipping routes. By shifting trade flows to alternative channels, firms succeed in sustaining their overall export structure. This evidence aligns with our findings in subsubsection 7.3.2, confirming that firms respond to climate risks primarily by restructuring logistics channels rather than withdrawing from export markets.

In summary, constrained by the inability to switch transport modes, firms resort to a hierarchy of second-best adjustments. We document that spatial arbitrage (route

switching) and market diversion (domestic sales) serve as pervasive "escape valves" to mitigate revenue losses across the board. In contrast, intertemporal substitution (inventory accumulation) exhibits strict conditionality: it functions as an effective hedge only for non-time-sensitive goods. For time-sensitive products, the prohibitive shadow cost of delay effectively shuts down this inventory channel, leaving firms with limited recourse but to absorb the quantity rationing through reduced trade volumes. This heterogeneity underscores that product attributes—specifically perishability—determine the firm's capacity to smooth infrastructure shocks.

8 Conclusion

This paper characterizes the fragility of global trade networks through the lens of specific transport infrastructure. By integrating granular hydrological, vessel-movement, and firm-level data, we document how climate shocks propagate not through production damages, but through the severance of physical connectivity. Our analysis yields three structural insights.

First, we establish that infrastructure rigidities transform hydrological anomalies into quantity rationing mechanisms. Unlike standard trade cost shocks that clear markets through prices, drought-induced capacity constraints create a logistical squeeze. The resulting shadow cost of congestion acts as a wedge that crowds out trade volumes, particularly for financially constrained firms and those exporting time-sensitive goods.

Second, we identify the limits of adaptation under modal lock-in. Contrary to the assumption of frictionless intermodal substitution, we find that firms are effectively locked into the waterway network due to prohibitive switching costs. This failure of arbitrage forces agents into a hierarchy of second-best resource reallocations: firms substitute intertemporally (inventory accumulation) and spatially (domestic market diversion) rather than switching transport modes. While these strategies buffer revenue, they represent a constrained optimization that deviates from the efficient trade equilibrium.

Finally, our findings bear broader implications for infrastructure resilience. As climate change intensifies the volatility of river systems, the reliance on single-mode transport corridors becomes a systemic vulnerability. The "double shock" of physical bottlenecks and financial amplification suggests that resilience requires not just infrastructure investment (e.g., dredging), but also institutional flexibility—such as multimodal integration and supply chain finance—to relax the rigidity constraints that currently bind exporters.

References

Abatzoglou, J., Dobrowski, S., Parks, S., *et al.* 2018. TerraClimate, a high-resolution global dataset of monthly climate and climatic water balance from 1958–2015. *Scientific Data*, **5**, 170191.

Acemoglu, Daron, & Tahbaz-Salehi, Alireza. 2024. The Macroeconomics of Supply Chain Disruptions. *Review of Economic Studies*. Forthcoming.

Acemoglu, Daron, Akcigit, Ufuk, & Kerr, William. 2015. *Networks and the Macroeconomy: An Empirical Exploration*. Working Paper 21344. National Bureau of Economic Research.

Al-Ayyoub, Naser, & Phan, Hieu V. 2026. Riskier climate, closer ties? How climate risk drives firms towards bank debt financing. *Journal of Corporate Finance*, **89**(January), 103017.

Balboni, Clare. 2025. In harm's way? infrastructure investments and the persistence of coastal cities. *American Economic Review*, **115**(1), 77–116.

Barrot, Jean-Noël, & Sauvagnat, Julien. 2016. Input Specificity and the Propagation of Idiosyncratic Shocks in Production Networks. *The Quarterly Journal of Economics*, **131**(3), 1543–1592.

Benincasa, Emanuela, Betz, Frank, & Gattini, Luca. 2024. How do firms cope with losses from extreme weather events? *Journal of Corporate Finance*, **84**(February), 102004.

Bernstein, Asaf, Billings, Stephen B, Gustafson, Matthew T, & Lewis, Ryan. 2022. Partisan residential sorting on climate change risk. *Journal of Financial Economics*, **146**(2), 410–437.

Brancaccio, Giulia, Kalouptsidi, Myrto, & Papageorgiou, Theodore. 2025. Rigidities in Transportation and Supply Chain Disruptions. *AEA Papers and Proceedings*, **115**, 543–550.

Carvalho, Vasco M, Nirei, Makoto, Saito, Yukiko U, & Tahbaz-Salehi, Alireza. 2021. Supply Chain Disruptions: Evidence from the Great East Japan Earthquake. *The Quarterly Journal of Economics*, **136**(2), 1255–1321.

Chaijaroen, Pasita. 2019. Long-lasting income shocks and adaptations: Evidence from coral bleaching in Indonesia. *Journal of Development Economics*, **138**, 1–15.

Chiovelli, Giorgio, Michalopoulos, Stelios, & Papaioannou, Elias. 2025. Landmines and spatial development. *Econometrica*, **93**(5), 1897–1940.

Cohn, Jonathan B. 2022. *Count (and Count-like) Data in Finance*. Tech. rept. McCombs School of Business, University of Texas at Austin. Working Paper, August 2022.

Costinot, Arnaud, Donaldson, Dave, & Smith, Cory. 2016. Evolving Comparative Advantage and the Impact of Climate Change in Agricultural Markets: Evidence from 1.7 Million Fields around the World. *Journal of Political Economy*, **124**(1), 205–248.

Davis, Steven J, Qian, Meijun, & Zeng, Wen. 2025. A Comprehensive GIS Database for China's Surface Transport Network with Implications for Transport and Socioeconomics Research. *NBER Working paper*.

Hadlock, C. J., & Pierce, J. R. 2010. New Evidence on Measuring Financial Constraints: Moving beyond the KZ Index. *Review of Financial Studies*, **23**, 1909–1940.

Hansen-Lewis, Jamie. 2026. Air pollution and manufacturing productivity: Understanding the roles of technology and adaptation. *Journal of Development Economics*, **160**(February), 103124.

Harris, Ian, Osborn, Timothy J., Jones, Phil, & Lister, David. 2020. Version 4 of the CRU TS monthly high-resolution gridded multivariate climate dataset. *Scientific Data*, **7**(1), 109.

Hong, Harrison, Wang, Neng, & Yang, Jinqiang. 2023. Mitigating Disaster Risks in the Age of Climate Change. *Econometrica*, **91**(5), 2015–2062.

Känzig, Diego R, & Raghavan, Ramya. 2025. *The Macroeconomic Effects of Supply Chain Shocks: Evidence from Global Shipping Disruptions*. Unpublished Manuscript. Working Paper.

Nath, Ishan. 2025. Climate Change, the Food Problem, and the Challenge of Adaptation through Sectoral Reallocation. *Journal of Political Economy*.

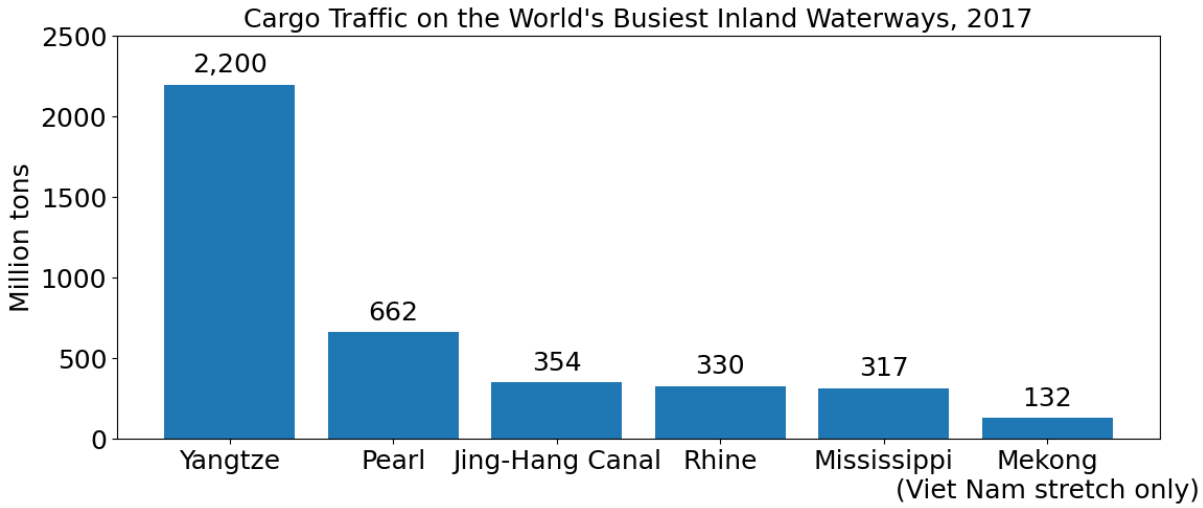
Silva, J. M. C. Santos, & Tenreyro, Silvana. 2006. The Log of Gravity. *The Review of Economics and Statistics*, **88**(4), 641–658.

Waldinger, Maria. 2025. The Economic Effects of Long-Term Climate Change: Evidence from the Little Ice Age. *Journal of Political Economy*. Forthcoming.

Yan, Denghua, Wang, Kun, Qin, Tianling, Weng, Baisha, Wang, Hao, Bi, Wuxia, Li, Xiangnan, Li, Meng, Lv, Zhenyu, Liu, Fang, *et al.* 2019. A data set of global river networks and corresponding water resources zones divisions. *Scientific Data*, **6**(1), 219.

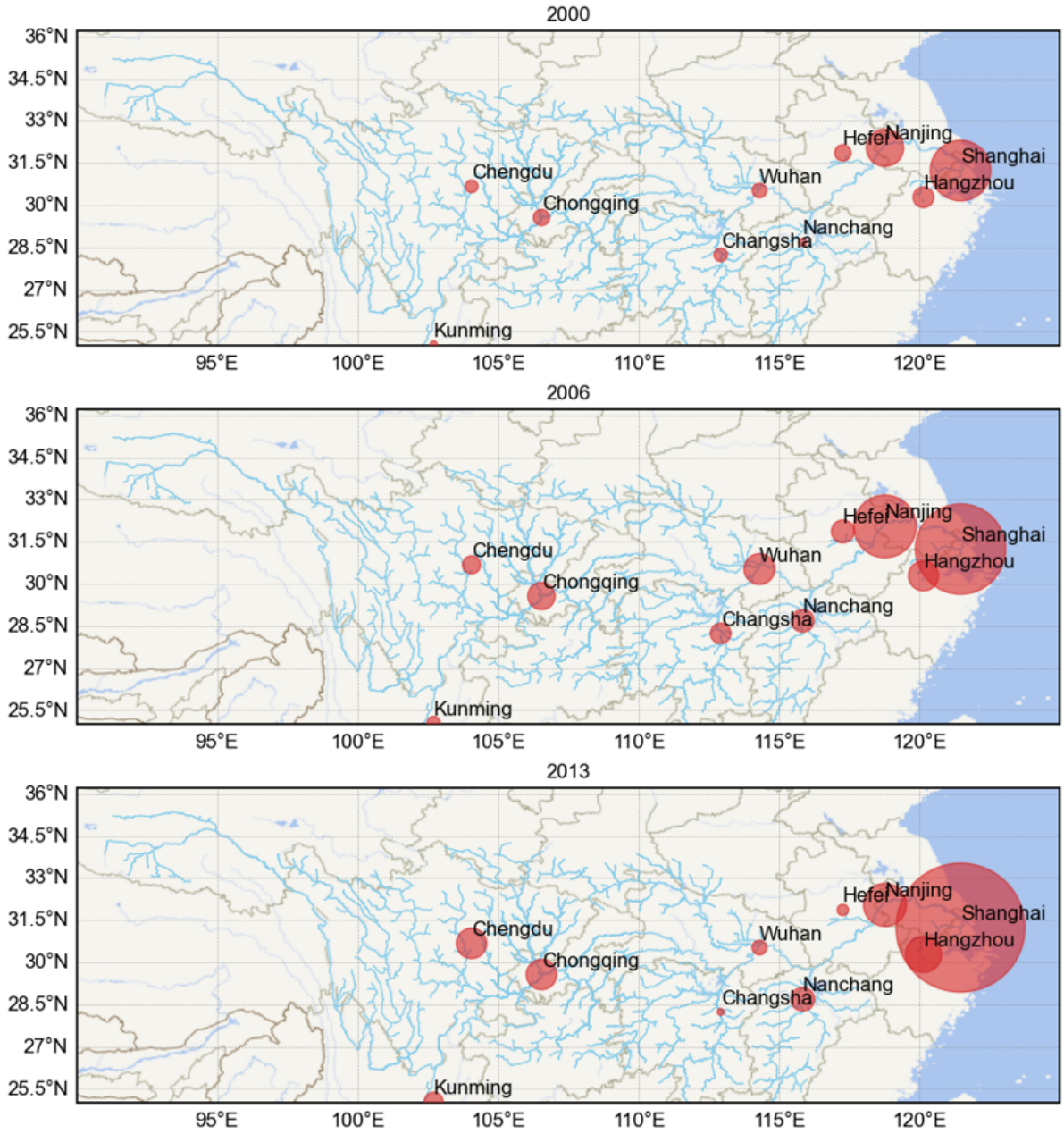
Figures and Tables

Figure 1: Annual Cargo Throughput of Major Global Inland Waterways (2017)



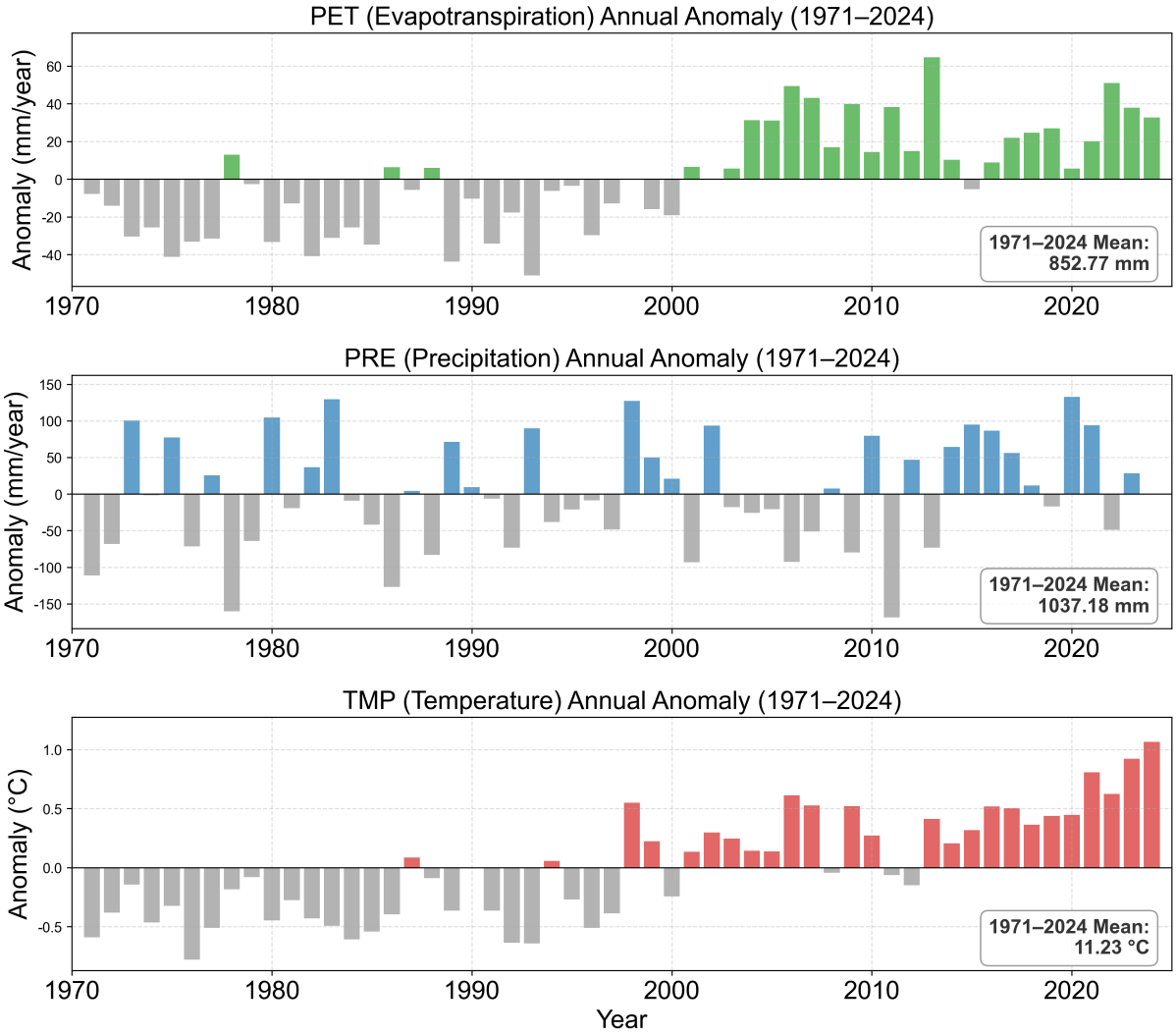
Notes: This figure plots the annual cargo volume (in million tons) for selected major inland waterways, including the Yangtze River, Beijing-Hangzhou Grand Canal, Rhine River, Mississippi River, and Mekong River. Data for the Mekong River is restricted to the section within Vietnam. Sources: Authors' compilation based on data from the Yangtze River Administration, Pearl River Water Resources Commission, and relevant international official statistics.

Figure 2: Spatial Distribution of Customs Port Cities in the Yangtze River Basin



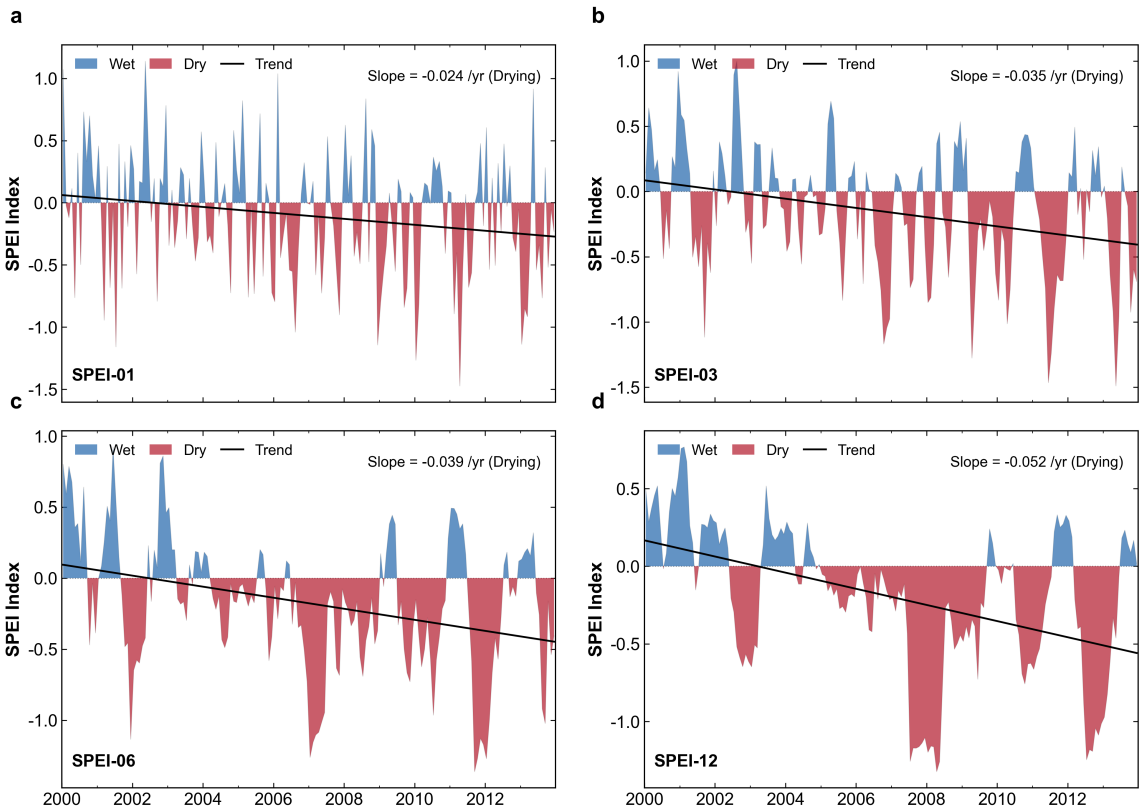
Notes: This figure displays the geographic distribution of customs port cities in the Yangtze River Basin that reported positive export records in all three benchmark years: 2000, 2006, and 2013. The base map is sourced from Tianditu (Map World), overlaid with the main stream and major tributaries of the Yangtze River. Red circles represent the total value of waterway exports for each city, with circle areas scaled proportionally to the square root of the export value. City names are labeled in English.

Figure 3: Annual Climate Anomalies in the Yangtze River Basin (1971–2024)



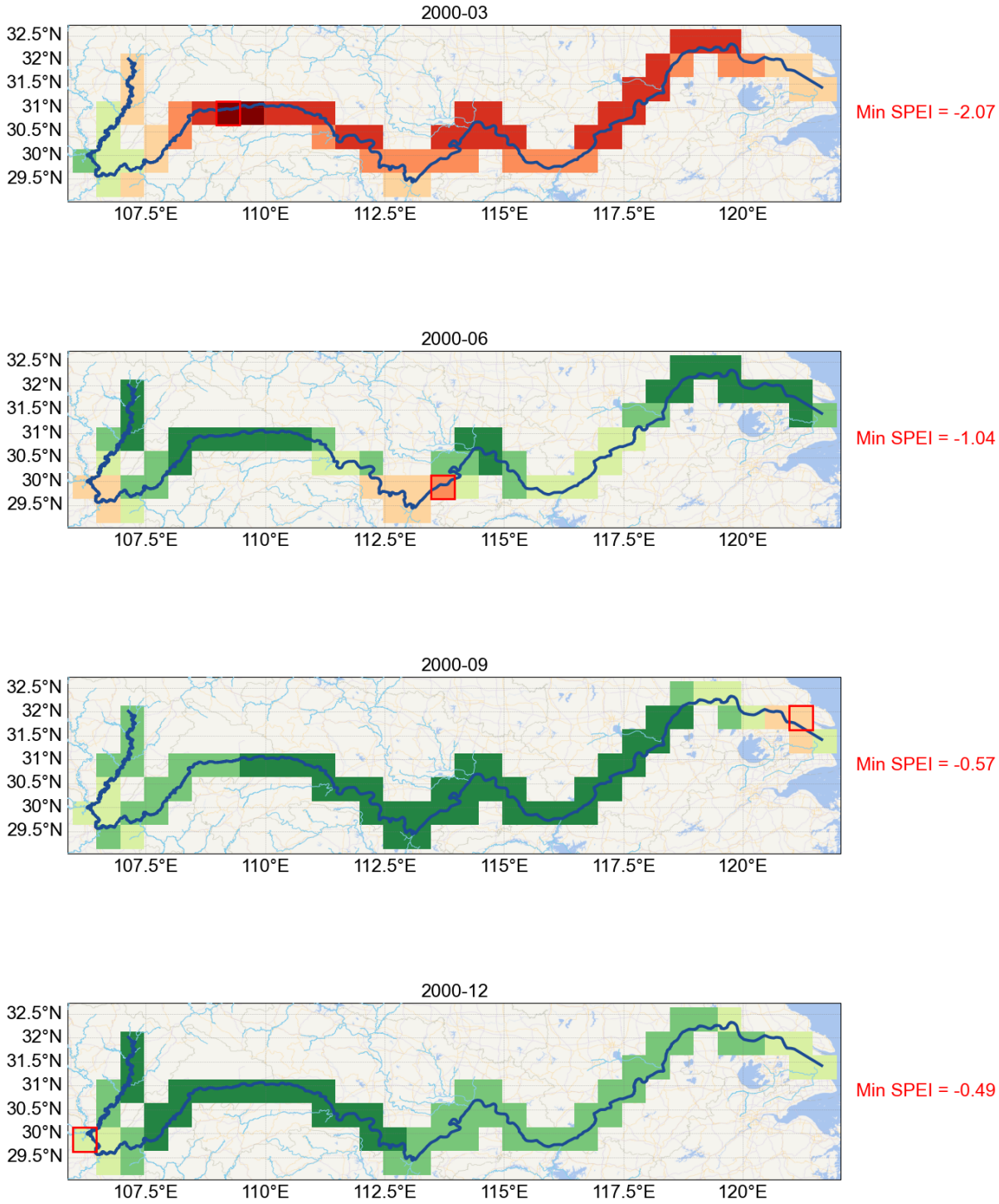
Notes: This figure plots the annual anomalies for three key climate indicators: Potential Evapotranspiration (PET), Precipitation (PRE), and Temperature (TMP). All variables are calculated as basin-wide averages. PET and PRE are derived from annual totals, while TMP is derived from annual means. Anomalies are defined as the deviation of each year's value from the 1971–2024 long-run mean. Positive (negative) values indicate levels above (below) the historical average.

FIGURE 4: DRYING TRENDS OF SPEI IN THE YANGTZE RIVER BASIN (2000-2013)



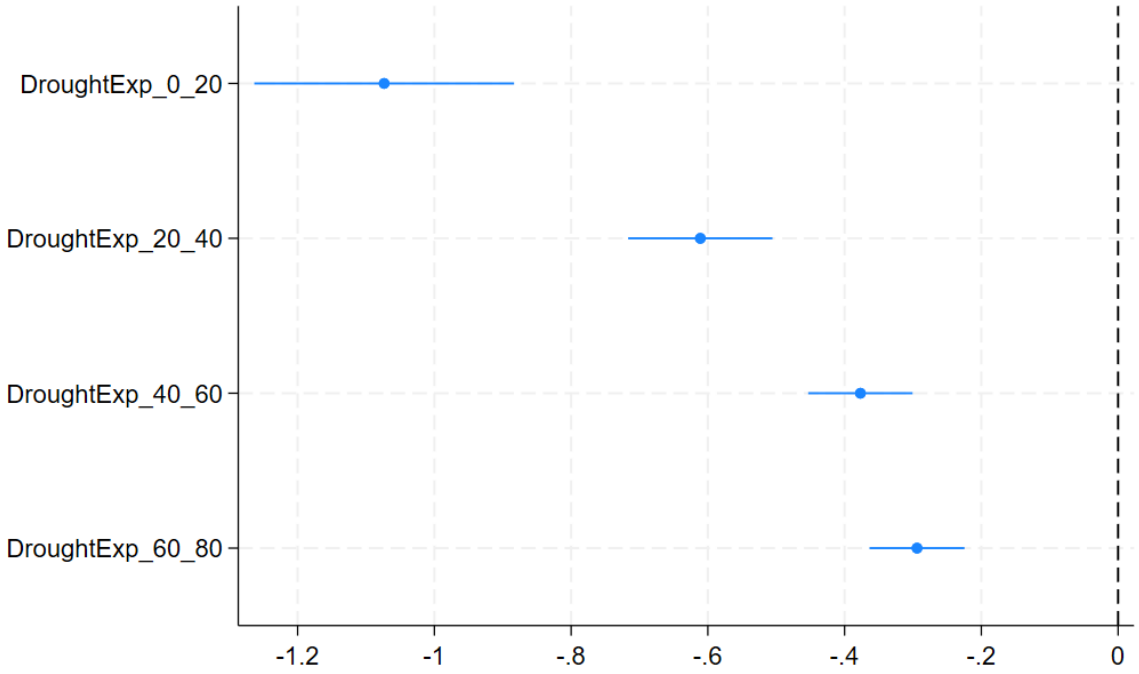
Notes: This figure illustrates the intensification of drought conditions during the sample period (2000-2013) by plotting the monthly time series of SPEI at 1-, 3-, 6-, and 12-month timescales. The solid black lines represent linear trends, with the calculated slopes indicating a consistent drying trend (negative slope) across all timescales.

Figure 5: Illustration of the Shortest Navigable Inland Waterway Route (Bazhong–Shanghai)



Notes: This figure illustrates the spatial configuration of the shortest navigable inland waterway route, using the trajectory from Bazhong to Shanghai as a representative example. The thick red line delineates the primary shipping channel along the Yangtze main stream, traversing 27 prefectural-level cities with a total navigable length of approximately 3,223.11 km. Colored grid cells indicate the spatial coverage of the shipping route within the raster dataset, while the blue line traces the specific shipment path. The grid cell highlighted by a red bounding box identifies the location with the most severe drought exposure (the "bottleneck") along the route for the given month.

FIGURE 6: ESTIMATED IMPACT OF DROUGHT EXPOSURE ON EXPORTS ACROSS SPEI QUANTILES



Notes: This figure plots the estimated coefficients (β_q) from equation (13), capturing the heterogeneous effects of drought exposure on firm exports across different quantiles of drought exposure. The vertical axis denotes the specific quantile bins of route-level drought exposure ($DroughtExp$), while the horizontal axis displays the magnitude of the estimated impact. Solid circles represent point estimates for each quantile bin, and horizontal bars indicate 95 percent confidence intervals. The regression specification controls for year fixed effects and firm-route fixed effects.

Table 1: Summary Statistics

Variable	N	Mean	SD	Min	Max
$Export_{value}$	100,177	4.205e+03	1.078e+04	0	7.554e+04
$Export_{CountryType}$	100,177	7.037	9.433	0	47
$Export_{GoodsType}$	100,177	5.146	7.797	0	45
$DroughtExp$	100,177	-0.446	0.334	-1.680	0.122
$DroughtExp_{2015}$	100,177	-0.446	0.334	-1.680	0.122
$DroughtExp_{avg01}$	100,177	-0.164	0.230	-0.852	0.351
$DroughtExp_{min03}$	100,177	-0.530	0.472	-2.307	0.449
$DroughtExp_{min06}$	100,177	-0.597	0.579	-2.031	0.697
$DroughtExp_{min12}$	100,177	-0.770	0.586	-2.166	0.548
$DroughtExpWeight_{avg01}$	100,177	-0.162	0.231	-0.852	0.368
$DroughtExpWeight_{min01}$	100,177	-0.283	0.167	-1.022	0.00589
$DroughtExp_{upstream}$	100,177	-1.911	0.142	-2.105	-1.597
$DroughtExp_{industry}$	99,901	-0.155	0.275	-0.903	0.531
Lev	88,399	0.558	0.232	0.0100	1.146
$ln(Assets)$	100,177	10.97	1.555	0.693	15.28
Age	100,177	9.652	8.182	0	49
ROE	84,812	0.246	0.388	0	2.502
$Production$	81,237	283,466	666,894	3	4.769e+06
$SalesRevenue$	88,403	272,574	656,376	32	4.723e+06
$SalesCosts$	88,398	229,717	560,263	29	4.065e+06
$Overheads$	88,399	11,623	26,179	1	186,327
$Inventory$	88,329	34,078	83,859	0	593,552
$FinishedGoods$	87,694	12,585	30,644	0	211,133
$IndustrialSales$	81,236	277,655	654,855	1	4.674e+06

Notes: This table presents summary statistics for the main variables used in the analysis. The sample is constructed at the firm-route-year level, comprising 100,177 observations. To mitigate the influence of outliers, all continuous variables are winsorized at the 1st and 99th percentiles, and observations with anomalous zero values are excluded. Detailed variable definitions and construction methods are provided in Section section 4. Monetary values are expressed in thousands of RMB.

Table 2: Baseline Estimates: The Impact of Drought Exposure on Firm Exports

	$Export_{value}$	
	(1)	(2)
DroughtExp	0.5554***	0.5902***
	(0.091)	(0.096)
Observations	100,177	84,811
Pseudo-R2	0.8505	0.8617
Control	NO	YES
Year FE	YES	YES
Firm-Route FE	YES	YES
Cluster	Firm	Firm

Notes: This table reports the baseline regression results estimated using the Poisson Pseudo Maximum Likelihood (PPML) estimator. The dependent variable is the annual export value of a firm on a given route. The key explanatory variable, *DroughtExp*, measures route-level annual drought exposure, constructed based on the maximum drought severity observed in the grid cells traversed by the route. Column (1) presents the baseline specification without firm-level controls. Column (2) includes firm-level controls: leverage ratio, total assets, firm age, and return on assets (ROA). All specifications include year fixed effects and firm-route fixed effects. Robust standard errors clustered at the firm level are reported in parentheses. *** p<0.01, ** p<0.05, * p<0.1.

Table 3: Controlling for Potential Confounders

	$Export_{value}$					
	(1)	(2)	(3)	(4)	(5)	(6)
$DroughtExp$	0.5694***	0.6008***	0.5983***	0.6606***	0.8095***	0.7922***
	(0.094)	(0.098)	(0.094)	(0.100)	(0.111)	(0.117)
$DroughtExp_{upstream}$	-1.9515**	-1.6877				
	(0.863)	(1.154)				
$Upflow$			-0.0013***	-0.0026***	0.0020***	-0.0004
			(0.001)	(0.001)	(0.001)	(0.001)
$DroughtExp_{industry}$					-0.2692***	-0.1818***
					(0.048)	(0.055)
Observations	100,177	84,811	100,177	84,811	99,901	84,600
Pseudo-R2	0.851	0.862	0.851	0.862	0.851	0.862
Control	NO	YES	NO	YES	No	YES
Year FE	YES	YES	YES	YES	YES	YES
Firm-Route FE	YES	YES	YES	YES	YES	YES
Cluster	Firm	Firm	Firm	Firm	Firm	Firm

Notes: This table presents robustness checks by augmenting the baseline model with controls for potential confounding factors. The dependent variable is the firm's annual export value on a given route. The key explanatory variable, $DroughtExp$, measures route-level annual drought exposure. $DroughtExp_{upstream}$ denotes the average drought exposure in the upstream watershed of the shipping route. $DroughtExp_{factory}$ captures the drought conditions at the firm's production location. All specifications include year fixed effects and firm-route fixed effects. Robust standard errors clustered at the firm level are reported in parentheses. *** p<0.01, ** p<0.05, * p<0.1.

Table 4: Impact of Drought on Vessel Navigation Behavior (AIS Data)

	StayDuration		*VoyageDuration*	
	(1)	(2)	(3)	(4)
$DroughtExp_{L1}$	-0.0324***	0.0145		
	(0.010)	(0.011)		
$DroughtExp_{L1} \times Length$		-0.0810***		
		(0.006)		
$DroughtExp$			-0.2522***	-0.2171***
			(0.007)	(0.008)
$DroughtExp \times Length$				-0.0502***
				(0.004)
Observations	429,905	429,905	429,905	429,905
Pseudo-R2	0.413	0.414	0.354	0.355
Year-Month FE	YES	YES	YES	YES
Ship FE	YES	YES	YES	YES
Cluster	Ship	Ship	Ship	Ship

Notes: This table examines the impact of drought shocks on vessel navigation behavior using Automatic Identification System (AIS) data. The dependent variables are vessel port dwell time (*StayDuration*) and voyage duration (*VoyageDuration*). The key explanatory variable is the one-period lagged drought exposure ($DroughtExp_{L1}$). To capture heterogeneous effects, we introduce an interaction term with vessel length (*Length*). All specifications control for vessel fixed effects and year-month fixed effects. Robust standard errors clustered by Maritime Mobile Service Identity (MMSI) are reported in parentheses. *** p<0.01, ** p<0.05, * p<0.1.

Table 5: Impact of Drought Shocks on Firm Cost Structure

	$SalesCosts/IndustrialSales$		$Overheads/IndustrialSales$	
	(1)	(2)	(3)	(4)
$DroughtExp$	-1.5349***	-1.6499***	-1.2161**	-1.2833**
	(0.404)	(0.433)	(0.517)	(0.540)
Observations	69,528	66,333	69,529	66,334
Pseudo-R2	0.708	0.718	0.271	0.278
Control	NO	YES	NO	YES
Year FE	YES	YES	YES	YES
Firm FE	YES	YES	YES	YES
Cluster	Firm	Firm	Firm	Firm

Notes: This table investigates the effects of drought shocks on the cost structure of firms. The dependent variables are the ratio of sales costs to industrial sales ($SalesCosts/IndustrialSales$) and the ratio of overhead expenses to industrial sales ($Overheads/IndustrialSales$). The key explanatory variable, $DroughtExp$, denotes the firm-level average drought exposure, calculated as the weighted average of annual drought exposure across all export routes utilized by the firm. All specifications include firm fixed effects and year fixed effects. Robust standard errors clustered at the firm level are reported in parentheses. *** p<0.01, ** p<0.05, * p<0.1.

Table 6: The Moderating Role of Financial Constraints

	$Export_{value}$	
	(1)	(2)
$DroughtExp$	1.0356***	1.2844***
	(0.137)	(0.171)
SA	1.0566***	1.0513***
	(0.100)	(0.111)
$DroughtExp \times SA$	0.2204***	0.2831***
	(0.030)	(0.042)
Observations	85,871	71,832
Pseudo-R2	0.864	0.866
Control	NO	YES
Year FE	YES	YES
Firm FE	YES	YES
Cluster	Firm	Firm

Notes: This table examines how financial constraints modulate the impact of drought shocks on firm exports. The dependent variable is the firm's annual export value. The key explanatory variable is firm-level drought exposure ($DroughtExp$). The financial constraint indicator, SA, is the Size-Age index constructed following Hadlock & Pierce (2010), where higher values indicate more severe financial constraints. The interaction term $DroughtExp \times SA$ is included to identify the amplifying effect of credit constraints. All specifications include firm fixed effects and year fixed effects. Robust standard errors clustered at the firm level are reported in parentheses. *** p<0.01, ** p<0.05, * p<0.1.

Table 7: Adaptation via Intermodal Substitution: Switching to Railway and Highway

	$Export_{value}$	
	(1)	(2)
$DroughtExp$	0.4966***	0.3462**
	(0.103)	(0.151)
$SwitchToRailway \times DroughtExp$	-0.3980	
	(0.290)	
$SwitchToHighway \times DroughtExp$		0.1200
		(0.208)
Observations	71,832	71,832
Control	YES	YES
Year FE	YES	YES
Firm FE	YES	YES
Cluster	Firm	Firm
Pseudo R^2	0.872	0.872

Notes: This table examines whether firms adapt to drought shocks by switching transportation modes. The dependent variable is the firm' s annual export value. The key explanatory variable is firm-level drought exposure ($DroughtExp$). To capture potential intermodal substitution effects, we interact $DroughtExp$ with indices measuring the feasibility of switching to railway ($SwitchToRailway$) and highway ($SwitchToHighway$) transport. All specifications control for firm fixed effects and year fixed effects. Robust standard errors clustered at the firm level are reported in parentheses. *** p<0.01, ** p<0.05, * p<0.1.

Table 8: Interactions with Waterway Dependence and Time Sensitivity

	$Export_{value}$			
	(1)	(2)	(3)	(4)
$DroughtExp$	0.3566***	0.3746***	0.3494***	0.3570***
	(0.077)	(0.081)	(0.079)	(0.083)
$DroughtExp \times WaterwayDep$	0.0373	0.0687*		
	(0.031)	(0.041)		
$DroughtExp \times TimeSensitivity$			0.0530*	0.1150***
			(0.032)	(0.042)
Observations	85,871	71,832	85,871	71,832
Control	NO	YES	NO	YES
Year FE	YES	YES	YES	YES
Firm FE	YES	YES	YES	YES
Cluster	Firm	Firm	Firm	Firm
Pseudo R^2	0.859	0.872	0.859	0.872

Notes: This table examines the heterogeneous impacts of drought exposure by interacting $DroughtExp$ with firm/industry characteristics. The dependent variable is the firm' s annual export value on a given route. Columns (1)–(2) report interactions with $WaterwayDep$, an index measuring industry-level dependence on waterway transport intermediate inputs, derived from the 1997 Input-Output Table of China. Columns (3)–(4) report interactions with $TimeSensitivity$, a binary indicator classified via semantic analysis of product characteristics using the DeepSeek v3.1 Large Language Model. All specifications include firm fixed effects and year fixed effects. Robust standard errors clustered at the firm level are reported in parentheses. *** p<0.01, ** p<0.05, * p<0.1.

Table 9: Impact of Drought Shocks on Firm Production Activities

	$Production/IndustrialSales$		
	(1)	(2)	(3)
$DroughtExp$	-0.0071	-0.0047	-0.0031
	(0.011)	(0.011)	(0.011)
$DroughtExp \times WaterwayDep$		-0.0046	-0.0074
		(0.005)	(0.006)
$DroughtExp \times TimeSensitivity$			-0.0035
			(0.005)
$DroughtExp \times WaterwayDep \times TimeSensitivity$			0.0087
			(0.009)
Observations	66,336	66,336	66,336
Control	YES	YES	YES
Year FE	YES	YES	YES
Firm FE	YES	YES	YES
Cluster	Firm	Firm	Firm

Notes: This table examines the effect of drought shocks on firm production activities. The dependent variable is the production level, proxied by the ratio of gross industrial output value to industrial sales value. The key explanatory variable is the firm-level average drought exposure ($DroughtExp$). To explore heterogeneity, the specification is augmented with interaction terms involving waterway dependence ($WaterwayDep$) and time sensitivity ($TimeSensitivity$). All specifications include firm fixed effects and year fixed effects. Robust standard errors clustered at the firm level are reported in parentheses. *** p<0.01, ** p<0.05, * p<0.1.

Table 10: Inventory Adjustments in Response to Drought Shocks

	$Inventory/IndustrialSales$			$FinishedGoods/IndustrialSales$		
	(1)	(2)	(3)	(4)	(5)	(6)
$DroughtExp$	-1.3836***	-1.2314***	-0.8966**	-1.2372***	-1.0762***	-0.7809**
	(0.492)	(0.445)	(0.379)	(0.419)	(0.369)	(0.305)
$DroughtExp \times WaterwayDep$		-0.3149**	-0.6846***		-0.3259**	-0.6503***
		(0.147)	(0.206)		(0.163)	(0.215)
$DroughtExp \times TimeSensitivity$			-0.9384***			-0.8048***
			(0.275)			(0.264)
$DroughtExp \times WaterwayDep \times TimeSensitivity$			1.1510***			1.0102***
			(0.334)			(0.331)
Observations	66,318	66,318	66,318	65,985	65,985	65,985
Control	YES	YES	YES	YES	YES	YES
Year FE	YES	YES	YES	YES	YES	YES
Firm FE	YES	YES	YES	YES	YES	YES
Cluster	Firm	Firm	Firm	Firm	Firm	Firm

Notes: This table examines firm inventory adjustment behaviors in response to drought shocks. The dependent variables are the total inventory-to-sales ratio ($Inventory/IndustrialSales$) and the finished goods inventory-to-sales ratio ($FinishedGoods/IndustrialSales$). The key explanatory variable is the firm-level average drought exposure ($DroughtExp$). To capture heterogeneous effects, the model introduces interaction terms with waterway dependence and time sensitivity of goods. All specifications include firm fixed effects and year fixed effects. Robust standard errors clustered at the firm level are reported in parentheses. *** p<0.01, ** p<0.05, * p<0.1.

Table 11: Adaptation via Spatial Reallocation: Cross-Factory Production Shifting

	$Export_{value}$		
	(1)	(2)	(3)
$DroughtExp_{other}$	-2.1100**	-2.7298***	-2.3284**
	(0.975)	(1.016)	(1.108)
$DroughtExp_{other} \times WaterwayDep$		1.1116	0.9619
		(1.918)	(2.334)
$DroughtExp_{other} \times TimeSensitivity$			-0.8570
			(2.042)
$DroughtExp_{other} \times WaterwayDep \times TimeSensitivity$			0.3357
			(3.782)
$DroughtExp$	-0.1753	-0.1633	-0.1730
	(0.362)	(0.360)	(0.363)
Observations	4,493	4,493	4,493
Control	YES	YES	YES
Year FE	YES	YES	YES
Firm–Factory FE	YES	YES	YES
Cluster	Firm	Firm	Firm

Notes: This table examines firm adaptation through the spatial reallocation of production across internal factories. The analysis is conducted at the firm-factory-year level, with the dependent variable being the export value of a specific factory. The key explanatory variable, $DroughtExp_{other}$, measures the average drought exposure faced by the firm's other production facilities, constructed to identify cross-factory production shifting. Interaction terms with waterway dependence ($WaterwayDep$) and time sensitivity ($TimeSensitivity$) are included to capture heterogeneous responses. All specifications control for firm-factory fixed effects and year fixed effects. Robust standard errors clustered at the firm level are reported in parentheses. *** p<0.01, ** p<0.05, * p<0.1.

Table 12: Adaptation via Route Switching: Reallocating Exports across Customs Ports

	$Export_{value}$		
	(1)	(2)	(3)
$DroughtExp_{other}$	-1.2944***	-0.8907***	-0.7652***
	(0.181)	(0.212)	(0.279)
$DroughtExp_{other} \times WaterwayDep$		-0.7742**	-0.5735
		(0.329)	(0.392)
$DroughtExp_{other} \times TimeSensitivity$			-0.2359
			(0.403)
$DroughtExp_{other} \times WaterwayDep \times TimeSensitivity$			-0.7302
			(0.721)
$DroughtExp$	0.2847**	0.2873**	0.2610**
	(0.118)	(0.120)	(0.117)
Observations	35,469	35,469	35,469
Control	YES	YES	YES
Year FE	YES	YES	YES
Firm–Route FE	YES	YES	YES
Cluster	Firm	Firm	Firm

Notes: This table examines firm adaptation behavior through the adjustment of export customs ports (i.e., route switching). The dependent variable is the firm's export value on a given route. The key explanatory variable, $DroughtExp_{other}$, represents the drought exposure of alternative routes available to the firm, constructed to capture the potential for export path reconfiguration. The specification controls for the drought exposure of the current route ($DroughtExp$). Interaction terms with waterway dependence and time sensitivity of goods are included to explore heterogeneity. All specifications include firm-route fixed effects and year fixed effects. Robust standard errors clustered at the firm level are reported in parentheses. *** p<0.01, ** p<0.05, * p<0.1.

Table 13: Adaptation via Market Switching: Reallocating Sales to the Domestic Market

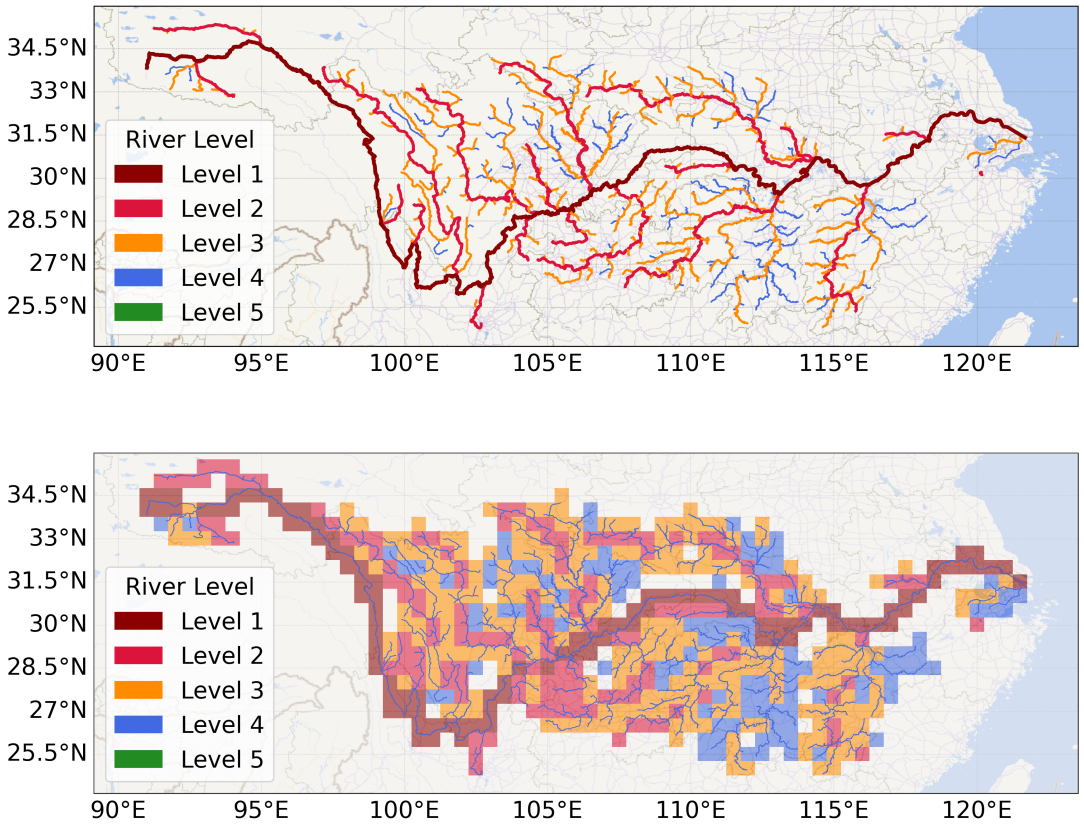
	DomesticSales		
	(1)	(2)	(3)
$DroughtExp$	-0.0143***	-0.0156***	-0.0147***
	(0.003)	(0.003)	(0.003)
$DroughtExp \times WaterwayDep$		0.0024	0.0029
		(0.002)	(0.002)
$DroughtExp \times TimeSensitivity$			-0.0019
			(0.003)
$DroughtExp \times WaterwayDep \times TimeSensitivity$			-0.0040
			(0.004)
Observations	66,336	66,336	66,336
Control	YES	YES	YES
Year FE	YES	YES	YES
Firm FE	YES	YES	YES
Cluster	Firm	Firm	Firm

Notes: This table examines firm market adjustment behaviors, specifically the shift from export markets to domestic sales, as a buffer against drought shocks. The dependent variable is the share of domestic sales ($DomesticSales$), defined as one minus the ratio of export value to industrial sales value ($1 - ExportValue/IndustrialSales$). The key explanatory variable is the firm-level average drought exposure ($DroughtExp$). Interaction terms are included to examine the moderating roles of waterway dependence and time sensitivity of goods on market adjustment behaviors. All specifications include firm fixed effects and year fixed effects. Robust standard errors clustered at the firm level are reported in parentheses. *** p<0.01, ** p<0.05, * p<0.1.

Appendix

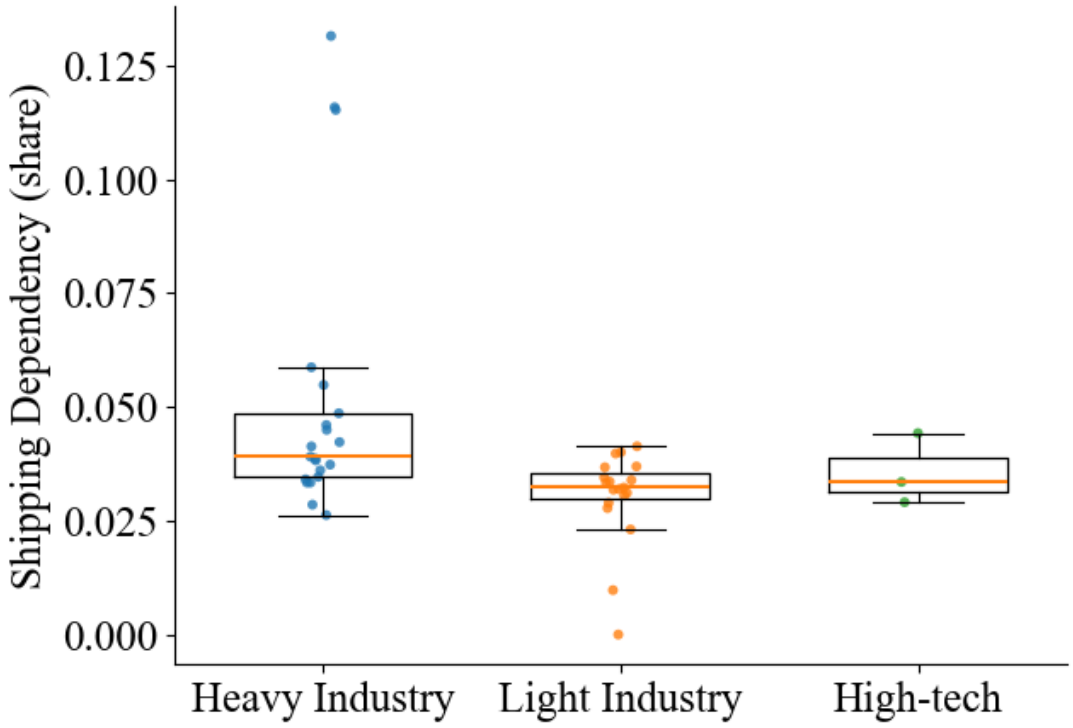
A Additional Tables and Figures

Figure A1: Spatial Distribution of Inland Waterway Grades in the Yangtze River Basin



Notes: This figure illustrates the spatial hierarchy of inland waterway grades, serving as the geographic basis for constructing waterway grade weights. The classification follows the Standard for Inland Waterway Navigation (GB 50139-2014), categorizing channels from Grade I to Grade V. The maximum permissible fleet dimensions (double-lane) for each grade are defined as follows: Grade I (250 m), Grade II (190 m), Grade III (110 m), Grade IV (90 m), and Grade V (70 m). Panels (a) and (b) present the spatial layout using distinct visualization schemes, where the color gradient from red to blue corresponds to Grade I through Grade V. This classification scheme underpins the calculation of drought exposure weights in the empirical analysis.

Figure A2: Distribution of Waterway Dependence across Industrial Sectors



Notes: This figure compares the distribution of waterway dependence across three broad industrial categories: Heavy Industry, Light Industry, and High-tech Manufacturing. The waterway dependence index is constructed using the 1997 Input-Output Table of China (124 sectors), defined as the share of intermediate inputs from the "Waterway Transport" sector relative to total transportation service inputs. In the boxplots, the rectangular box represents the interquartile range (IQR), and the horizontal line within the box marks the median. The whiskers extend to the most extreme data points within 1.5 times the IQR from the box edges.

Figure A3: API Configuration for Time Sensitivity Classification

```
response = client.chat.completions.create(
    model="Pro/deepseek-ai/DeepSeek-V3.1",
    messages=[
        {"role": "system", "content": "你是一位国际贸易和产业经济专家，擅长分析不同行业的出口特性。"},
        {"role": "user", "content": prompt}
    ],
    temperature=0.2,
    max_tokens=200
)
return response.choices[0].message.content.strip()
```

Notes: This figure displays the API parameter settings used to classify time sensitivity of goods via the DeepSeek-V3.1 Large Language Model. The system prompt primes the model to adopt the persona of an expert in international trade and industrial economics. To ensure the stability and reproducibility of the classification outcomes, the temperature parameter is set to 0.2. The maximum output length (max tokens) is restricted to 200.

Figure A4: Prompt Design for Identifying Product Time Sensitivity

```
prompt = f"""
请分析以下企业的主营业务，判断其出口订单的可调整难度是高还是低，并用0或1表示（0=低难度，1=高难度）。

企业名称：{enterprise_name}

企业业务信息：
{business_info}

判断标准（多维度综合评估）：
1. 产品时效性：
   - 高难度：生鲜食品、短期保鲜产品、季节性强的商品
   - 低难度：耐储存产品、无明显季节性的商品

2. 生产周期：
   - 高难度：生产周期长（数月或更长）、定制化生产
   - 低难度：生产周期短（数天至数周）、标准化生产

3. 库存特性：
   - 高难度：库存成本高、易损耗、库存周期短
   - 低难度：库存成本低、不易损耗、库存周期长

4. 贸易特性：
   - 高难度：依赖长期合同、大宗商品、专用设备
   - 低难度：短期合同为主、通用商品、标准化产品

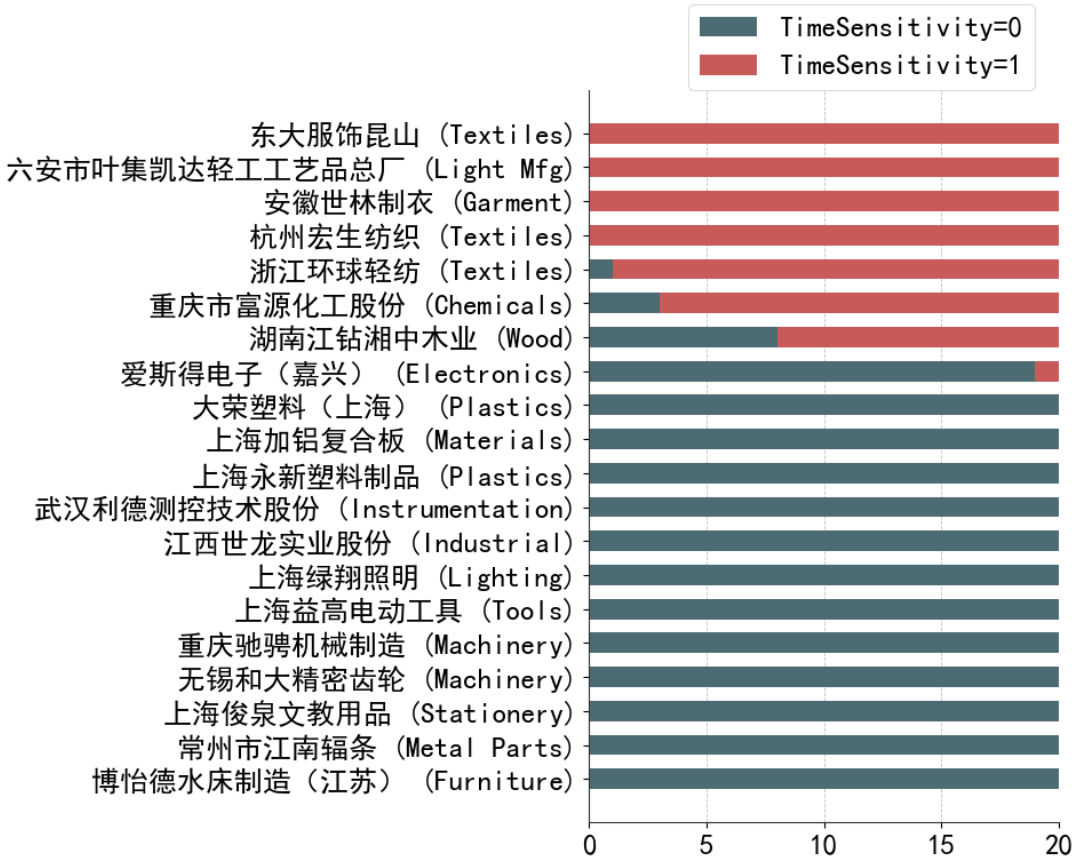
5. 市场适应性：
   - 高难度：产品用途单一、客户特定、转换成本高
   - 低难度：产品用途广泛、客户群体多样、转换成本低

分析步骤：
1. 总结该企业的核心业务和主要产品
2. 根据上述5个维度分析该企业产品的特性
3. 综合判断出口订单可调整难度是高(1)还是低(0)

输出格式（严格按照此格式输出，不要添加额外内容）：
业务概括：[用一句话概括企业的主要业务和产品]
可调整难度：[0或1]
"""
```

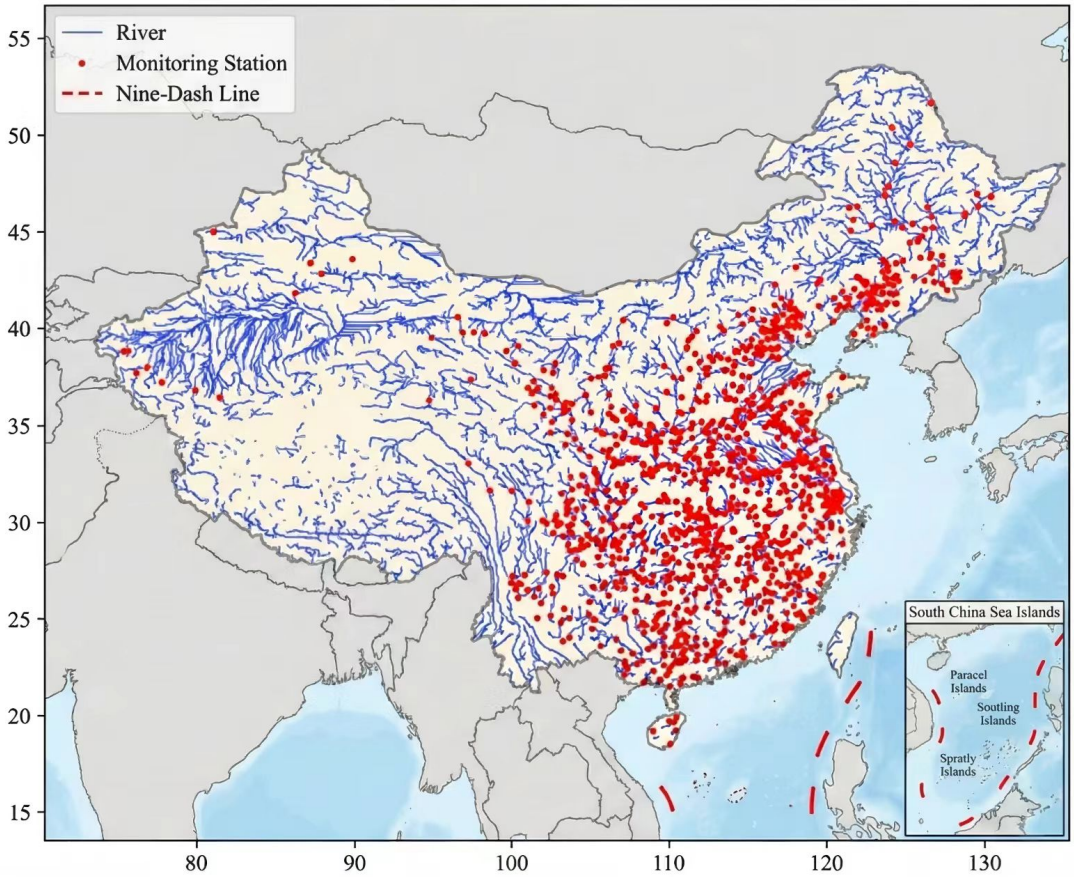
Notes: This figure illustrates the prompt engineering strategy used to classify the time sensitivity of commodities. The evaluation framework instructs the model to assess products across five comprehensive dimensions: product timeliness, production cycles, inventory characteristics, trade logistics organization, and market adaptability. The model is required to output results in a strictly standardized format, assigning a binary indicator where 0 denotes time-insensitive goods and 1 denotes time-sensitive goods.

FIGURE A5: STABILITY OF LLM-BASED TIME SENSITIVITY CLASSIFICATION



Notes: This figure evaluates the stability and consistency of the product time sensitivity classification derived from the Large Language Model. The analysis employs a random subsample of 20 firms, for which the classification procedure is repeated across 20 independent iterations. The horizontal axis indexes the iteration sequence (or trial round), while the vertical axis identifies the sample firms and their corresponding industrial sectors. Consistent results across iterations indicate high algorithmic stability.

Figure A6: Spatial Distribution of Hydrological Monitoring Stations in the Yangtze River Basin



Notes: The figure plots the geographic locations of major hydrological monitoring stations. The sample includes core stations situated along the main stem and primary tributaries. Data are sourced from the National Real-time Water Regime Monitoring System of the Ministry of Water Resources.

Table A1: Alternative Port Identification Standard

	$Export_{value}$	
	(1)	(2)
$DroughtExp_{2015}$	0.5535***	0.5881***
	(0.091)	(0.095)
Observations	100,240	84,867
Control	NO	YES
Year FE	YES	YES
Firm–Route FE	YES	YES
Cluster	Firm	Firm

Notes: This table reports robustness checks using an alternative identification standard for port terminals. The key explanatory variable, $DroughtExp_{2015}$, is recalculated based on the shipping route network identified via the Code for Ports of China (JT/T 24-2015), issued by the Ministry of Transport. Compared to the 2002 version used in the baseline analysis, this updated catalogue includes 29 additional inland ports. The dependent variable is the export value at the firm-route-year level. Column (1) excludes firm-level controls, while Column (2) controls for leverage ratio, total assets, firm age, and ROA. All specifications include year fixed effects and firm-route fixed effects. Robust standard errors clustered at the firm level are reported in parentheses. *** p<0.01, ** p<0.05, * p<0.1.

Table A2: Alternative Measures of Drought Exposure

	$Export_{value}$					
	(1)	(2)	(3)	(4)	(5)	(6)
$DroughtExp_{avg01}$	0.6622***					
	(0.114)					
$DroughtExpWeighted_{avg01}$		0.5676***				
		(0.107)				
$DroughtExpWeighted_{min01}$			0.3689**			
			(0.158)			
$DroughtExp_{min03}$				0.4507***		
				(0.086)		
$DroughtExp_{min06}$					0.1815***	
					(0.045)	
$DroughtExp_{min12}$						-0.0403
						(0.050)
Observations	84,811	84,811	84,811	84,811	84,811	84,811
Control	YES	YES	YES	YES	YES	YES
Year FE	YES	YES	YES	YES	YES	YES
Firm–Route FE	YES	YES	YES	YES	YES	YES
Cluster	Firm	Firm	Firm	Firm	Firm	Firm

Notes: This table reports robustness checks using various alternative drought exposure indices to verify the reliability of the baseline findings. The alternative measures are categorized into three groups: (1) Spatial Aggregation: $DroughtExp_{avg01}$ denotes the average 1-month SPEI across grid cells covered by the route (in contrast to the minimum value used in the baseline). (2) Waterway Weighting: $DroughtExpWeighted_{avg01}$ and $DroughtExpWeighted_{min01}$ incorporate waterway grade weights based on the Standard for Inland Waterway Navigation (GB 50139-2014), calculated as the weighted average and weighted minimum of route-level SPEI, respectively. (3) Temporal Scales: $DroughtExp_{min03}$, $DroughtExp_{min06}$, and $DroughtExp_{min12}$ represent the minimum route-level SPEI measured over 3-month, 6-month, and 12-month time horizons, respectively. The dependent variable is export value at the firm-route-year level. All specifications control for firm-level characteristics, year fixed effects, and firm-route fixed effects. Robust standard errors clustered at the firm level are reported in parentheses. *** p<0.01, ** p<0.05, * p<0.1.

Table A3: Sensitivity to Route Length (Number of Cities Traversed)

	$Export_{value}$		
	(1)	(2)	(3)
DroughtExp	1.3749***	0.5332***	0.6155***
	(0.233)	(0.104)	(0.109)
Observations	118,768	73,449	71,082
Control	YES	YES	YES
Year FE	YES	YES	YES
Firm–Route FE	YES	YES	YES
Cluster	Firm	Firm	Firm
Cities	>1	>3	>4

Notes: This table conducts robustness checks based on different route length screening criteria to mitigate potential biases arising from path distance characteristics. The dependent variable is the firm's export value, and the key explanatory variable is route-level drought exposure (*DroughtExp*). Columns (1), (2), and (3) report regression results for subsamples restricted to routes traversing more than 1, 3, and 4 cities, respectively. All specifications control for firm-level characteristics, year fixed effects, and firm-route fixed effects. Robust standard errors clustered at the firm level are reported in parentheses. *** p<0.01, ** p<0.05, * p<0.1.

Table A4: Placebo Test: Analysis of the Yellow River Basin

	$Export_{value}$	
	(1)	(2)
DroughtExp	1.2330	2.1171
	(2.079)	(2.113)
Observations	571	544
Control	No	Yes
Year FE	Yes	Yes
Firm-Route FE	Yes	Yes
Cluster	Firm	Firm

Notes: This table reports the results of a placebo test conducted using the Yellow River Basin sample, designed to rule out potential confounders driven by macro-climatic trends or regional common factors. The empirical strategy —including sample matching, variable construction, and estimation methods—mirrors the baseline analysis of the Yangtze River Basin, with the sole distinction being the geographic focus. The dependent variable is the export value at the firm-route-year level. Column (1) excludes firm-level controls, while Column (2) includes them. All specifications control for year fixed effects and firm-route fixed effects. Robust standard errors clustered at the firm level are reported in parentheses. *** p<0.01, ** p<0.05, * p<0.1.

Table A5: Impact on Export Loading Scale

	$Goods_{num}$		$Goods_{avg}$	
	(1)	(2)	(3)	(4)
DroughtExp	0.1968***	0.2264***	0.2330***	0.2938***
	(0.068)	(0.066)	(0.063)	(0.062)
Observations	869,531	648,228	869,531	648,228
Pseudo-R2	0.831	0.851	0.798	0.820
Control	NO	YES	NO	YES
Year FE	YES	YES	YES	YES
Firm-Route-Goods FE	YES	YES	YES	YES
Cluster	Firm	Firm	Firm	Firm

Notes: This table examines the transmission mechanism of drought shocks affecting firm export loading scale. The dependent variables are the total annual export quantity ($Goods_{num}$) and the average quantity per shipment ($Goods_{avg}$), with the latter serving as a proxy for the average vessel loading scale. The key explanatory variable, *DroughtExp*, measures route-level drought exposure. All specifications control for firm-level characteristics, year fixed effects, and firm-route-product fixed effects to rigorously absorb product heterogeneity and time-invariant route features. Robust standard errors clustered at the firm level are reported in parentheses. *** p<0.01, ** p<0.05, * p<0.1.

Table A6: Cost Pass-through via Export Prices

	Price	
	(1)	(2)
DroughtExp	-0.2054	-0.2249
	(0.141)	(0.161)
Observations	396,575	330,393
Pseudo-R2	0.993	0.994
Control	NO	YES
Year FE	YES	YES
Firm-Goods FE	YES	YES
Cluster	Firm	Firm

Notes: This table tests the price pass-through mechanism, examining whether firms pass on drought-induced cost pressures to downstream markets. The dependent variable is the average export unit value (*Price*), calculated at the firm-product-year level. The key explanatory variable, *DroughtExp*, measures firm-level average drought exposure. All specifications control for year fixed effects and firm-product fixed effects. Column (1) excludes firm-level controls, while Column (2) includes them. Robust standard errors clustered at the firm level are reported in parentheses. *** p<0.01, ** p<0.05, * p<0.1.

Table A7: Impact of Drought on River Water Levels

	$Waterlevel$
	(1)
$DroughtExp$	0.2188***
	(0.018)
Observations	11,160
R-squared	0.091
Year-Month FE	Yes
Station FE	Yes
Cluster	Station

Notes: This table provides empirical evidence for the shipping channel mechanism by examining the direct impact of drought shocks on river water levels. The dependent variable, $Waterlevel$, denotes the monthly water level recorded at major hydrological monitoring stations in the Yangtze River Basin. Data are obtained from the National Real-time Water Regime Monitoring Center of the Ministry of Water Resources, covering the period from July 2021 to December 2023. The key explanatory variable, $DroughtExp$, is the concurrent Standardized Precipitation Evapotranspiration Index (SPEI) calculated for the grid cell where the monitoring station is located. All specifications include year-month fixed effects (to absorb common time-varying shocks) and station fixed effects (to control for time-invariant geographic characteristics). Robust standard errors clustered at the station level are reported in parentheses. *** p<0.01, ** p<0.05, * p<0.1.

Table A8: Summary Statistics of Vessel-Level Variables (AIS Data)

Variable	N	Mean	SD	Min	Max
$StayDuration$	429,905	126.688	248.968	3.005	1,731.343
$VoyageDuration$	429,905	81.421	122.040	3.008	604.581
$DroughtExp$	429,905	-0.348	1.103	-2.596	1.731
$DroughtExp_{L1}$	429,905	-0.412	1.049	-2.596	1.816
$Length$	429,905	70.945	31.602	13.000	199.950

Notes: This table reports summary statistics for the main variables used in the vessel-level analysis. The sample is constructed using high-frequency (second-level) Automatic Identification System (AIS) data provided by the China Economic Information Service (CEIS) of Xinhua News Agency. We restrict the sample to cargo vessels operating in the Yangtze River Basin between January 2021 and November 2022. Following data cleaning and voyage identification procedures, the final sample comprises 429,905 observations at the vessel-year-month level. The main variables include port dwell time ($StayDuration$), average sailing speed ($AvgSpeed$), concurrent drought exposure ($DroughtExp$), one-period lagged drought exposure ($DroughtExp_{L1}$), and vessel length ($Length$). To mitigate the influence of outliers, all continuous variables are winsorized at the 99th percentiles, and observations with anomalous zero values are excluded.

Table A9: Summary Statistics of Firm-Level Variables

Variable	N	Mean	SD	Min	Max
$Export_{value}$	85,871	4.905e+03	1.160e+04	0	1.511e+04
$Export_{Country}$	85,871	9.889	11.89	1	165
$Export_{Goods}$	85,871	7.605	12.68	0	546
$DroughtExp$	85,871	-0.447	0.330	-1.680	0.122
Lev	75,192	0.557	0.233	0.0100	1.146
$ln(Assets)$	85,871	10.93	1.531	0.693	15.28
Age	85,871	9.396	7.852	0	49
ROE	71,833	0.248	0.390	0	2.502
$Production$	69,535	269,694	644,132	3	4.769e+06
$SalesRevenue$	75,196	258,950	632,336	32	4.723e+06
$SalesCosts$	75,191	218,309	539,954	29	4.065e+06
$Overheads$	75,192	10,896	24,705	1	186,327
$Inventory$	75,123	31,937	79,531	0	593,552
$FinishedGoods$	74,512	11,850	29,259	0	211,133
$IndustrialSales$	69,534	264,160	632,501	1	4.674e+06

Notes: This table reports summary statistics for core variables at the firm-year level. The final sample comprises 85,871 observations covering the period from 2000 to 2013. The main variables are categorized into three groups: (1) Trade variables, including export value ($Export_value$), number of export destinations ($Export_Country$), and number of export product varieties ($Export_Goods$); (2) Climate variables, specifically the firm-level average drought exposure ($DroughtExp$); and (3) Firm characteristics, covering leverage ratio (Lev), total assets ($Assets$), firm age (Age), industrial output, cost structure, and inventory levels. To mitigate the influence of outliers, all continuous variables are winsorized at the 99th percentiles, and observations with anomalous zero values are excluded. Monetary values are expressed in thousands of RMB.

Table A10: Lagged Effects of Drought Shocks on Firm Production Activities

Panel A

	Production/IndustrialSales		
	(1)	(2)	(3)
$DroughtExp_{L1}$	-0.0337	-0.0325	-0.0329
	(0.027)	(0.027)	(0.027)
$DroughtExp_{L1} \times WaterwayDep$		-0.0025	-0.0022
		(0.005)	(0.005)
$DroughtExp_{L1} \times TimeSensitivity$			0.0007
			(0.005)
$DroughtExp_{L1} \times WaterwayDep \times TimeSensitivity$			-0.0007
			(0.009)
Observations	66,336	66,336	66,336
Control	YES	YES	YES
Year FE	YES	YES	YES
Firm FE	YES	YES	YES
Cluster	Firm	Firm	Firm

Panel B

	Production/IndustrialSales		
	(4)	(5)	(6)
$DroughtExp_{L2}$	-0.0232	-0.0239	-0.0195
	(0.020)	(0.020)	(0.020)
$DroughtExp_{L2} \times WaterwayDep$		0.0013	-0.0031
		(0.005)	(0.005)
$DroughtExp_{L2} \times TimeSensitivity$			-0.0092
			(0.006)
$DroughtExp_{L2} \times WaterwayDep \times TimeSensitivity$			0.0098
			(0.009)
Observations	66,336	66,336	66,336
Control	YES	YES	YES
Year FE	YES	YES	YES
Firm FE	YES	YES	YES
Cluster	Firm	Firm	Firm

Notes: This table examines the lagged effects of drought shocks on firm production activities. The dependent variable is the production level, proxied by the ratio of gross industrial output value to industrial sales value ($Production/IndustrialSales$). The key explanatory variables are drought exposure lagged by one and two periods ($DroughtExp_{L1}$ and $DroughtExp_{L2}$). Interaction terms are included to identify the moderating roles of waterway dependence ($WaterwayDep$) and product time sensitivity ($TimeSensitivity$). All specifications include firm fixed effects, year fixed effects, and firm-level controls. Robust standard errors clustered at the firm level are reported in parentheses. *** p<0.01, ** p<0.05, * p<0.1.

Table A11: Comparison of Drought Effects across Different Panel Structures

	$Export_{value}$		
	(1)	(2)	(3)
DroughtExp	0.4083***	0.4348***	0.5902***
	(0.083)	(0.084)	(0.096)
Observations	71,832	74,171	84,811
Control	YES	YES	YES
Year FE	YES	YES	YES
Firm FE	YES	NO	NO
Firm–Factory FE	NO	YES	NO
Firm–Route FE	NO	NO	YES
Cluster	Firm	Firm	Firm

Notes: This table compares the estimated effects of drought shocks on firm exports across different panel data structures. The dependent variable is the firm's export value. The key explanatory variable is drought exposure (*DroughtExp*). Column (1) employs a firm-year panel and controls for firm fixed effects. Column (2) utilizes a firm-factory-year panel and includes firm-factory fixed effects. Column (3) is based on a firm-route-year panel with firm-route fixed effects. All specifications control for year fixed effects and firm-level characteristics. Robust standard errors clustered at the firm level are reported in parentheses. *** p<0.01, ** p<0.05, * p<0.1.

Table A12: Impact of Drought Shocks on Export Diversification

	$Export_{CountryType}$		
	(1)	(2)	(3)
DroughtExp	0.0642**	0.0706**	0.2011***
	(0.029)	(0.029)	(0.037)
Observations	71,832	74,171	84,811
Control	YES	YES	YES
Year FE	YES	YES	YES
Firm FE	YES	NO	NO
Firm–Factory FE	NO	YES	NO
Firm–Route FE	NO	NO	YES
Cluster	Firm	Firm	Firm

Notes: This table examines the impact of drought shocks on the diversification of firm export structures. The dependent variables are the number of export destination countries ($Export_{CountryType}$) and the number of export product varieties ($Export_{GoodsType}$). The key explanatory variable, *DroughtExp*, measures drought exposure at the route level. Columns (1)–(3) present results for the number of export destinations, while Columns (4)–(6) present results for the number of product varieties. To identify structural adjustments across different dimensions, the specifications employ varying levels of fixed effects: Columns (1) and (4) control for firm fixed effects; Columns (2) and (5) control for firm-factory fixed effects; and Columns (3) and (6) control for firm-route fixed effects. All models include year fixed effects and firm-level controls. Robust standard errors clustered at the firm level are reported in parentheses. *** p<0.01, ** p<0.05, * p<0.1.